Nano Research

ISSN 1998-0124 CN 11-5974/O4
https://doi.org/10.26599/NR.2026.94909280

Review Article

Hybrid bio-synthetic polymer gel electrolytes: Synergistic design and advanced applications for zinc-ion batteries

Adnan Ahmed[1], Muhammad Ali[2], Nishant Yadav[3], Yinchun Fang[1](✉), Xinhua Liu[1](✉)

[1] School of Textile and Garment, Anhui Polytechnic University, Wuhu 241000, China

[2] State Key Laboratory of Bio-based Fiber Materials, Zhejiang Sci-Tech University, Hangzhou 310018, China

[3] Department of Chemistry, Jaypee Institute of Information Technology, Noida, Uttar Pardesh, 201309, India

Nano Res., **Just Accepted Manuscript** • https://doi.org/10.26599/NR.2026.94909280

https://www.sciopen.com/journal/1998-0124 on Oct. 24, 2026

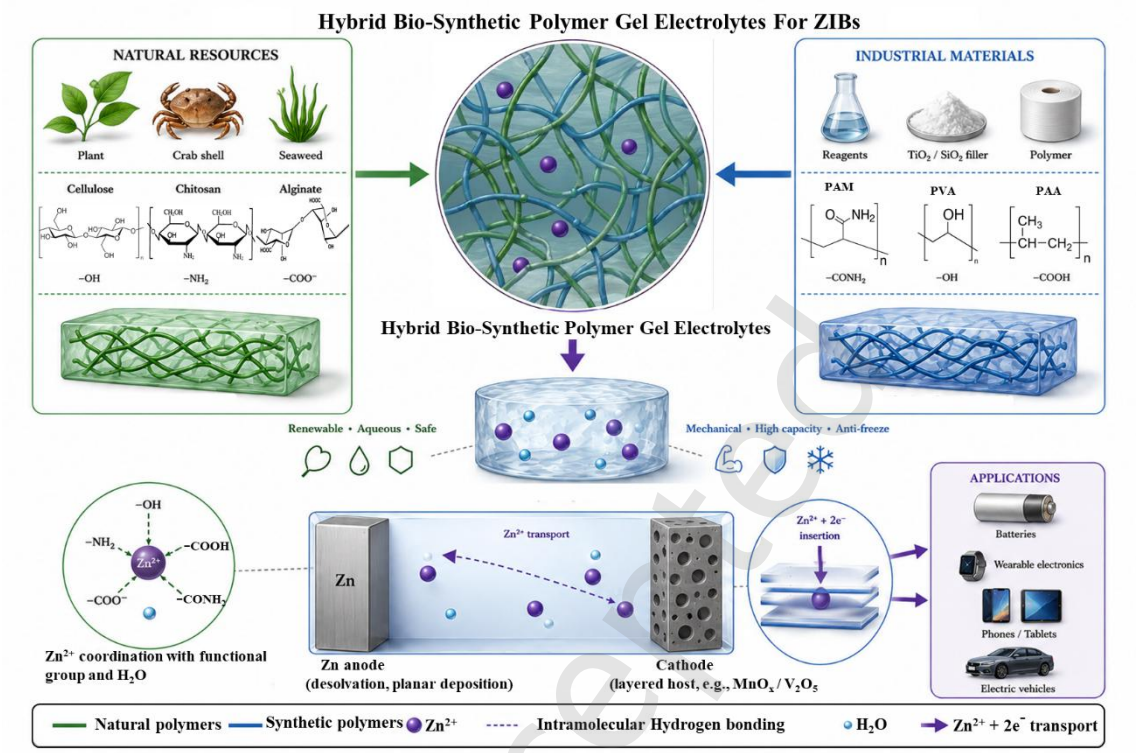
© The Authors(s)

Just Accepted

This is a "Just Accepted" manuscript, which has been examined by the peer-review process and has been accepted for publication. A "Just Accepted" manuscript is published online shortly after its acceptance,which is prior to technical editing and formatting and author proofing. Tsinghua University Press (TUP) provides "Just Accepted" as an optional and free service which allows authors to make their results available to the research community as soon as possible after acceptance. After a manuscript has been technically edited and formatted, and the page proofs have been corrected, it will be removed from the "Just Accepted" web site and published officially with volume and article number (e.g., *Nano Research*, **2025**, *18*, 94906990). Please note that technical editing may introduce minor changes to the manuscript text and/or graphics which may affect the content, and all legal disclaimers that apply to the journal pertain. In no event shall TUP be held responsible for errors or consequences arising from the use of any information contained in these "Just Accepted" manuscripts. To cite this anuscript please use its Digital Object Identifier (DOI®),which is identical for all formats of publication.

Just Accepted

TABLE OF CONTENTS (TOC)



This review summarizes recent advances in HB-SGs for zinc-ion batteries, focusing on network design, Zn^{2+} transport regulation, interfacial stabilization, and multifunctional performance. Additionally, key challenges and future perspectives regarding scalable manufacturing, practical implementation, and flexible energy storage are addressed.

Just Accepted

Review Article

Hybrid bio-synthetic polymer gel electrolytes: Synergistic design and advanced applications for zinc-ion batteries

Adnan Ahmed [1], Muhammad Ali [2], Nishant Yadav [3], Yinchun Fang [1] ✉, Xinhua Liu [1] ✉

[1] *School of Textile and Garment, Anhui Polytechnic University, Wuhu 241000, China*
[2] *State Key Laboratory of Bio-based Fiber Materials, Zhejiang Sci-Tech University, Hangzhou 310018, China*
[3] *Department of Chemistry, Jaypee Institute of Information Technology, Noida, Uttar Pardesh, 201309, India*

Received: 17 August 2026; **Revised:** 20 October 2026; **Accepted:** 24 October 2026

✉Address correspondence to Yinchun Fang, fangyc@ahpu.edu.cn; Xinhua Liu, liuxh@ahpu.edu.cn

Cite this article: *Nano Research*, 2026, 19, 94909280 https://doi.org/10.26599/NR.2026.94909280

ABSTRACT: Zinc-ion batteries (ZIBs) hold great promise for large-scale energy storage and wearable electronics owing to their high safety, raw material abundance, and environmental friendliness. However, conventional liquid electrolytes suffer from water decomposition, evaporation, and leakage, while zinc dendrites, anode corrosion, and hydrogen/oxygen evolution reactions further compromise battery stability. Polymer gel electrolytes mitigate these issues by forming hydrogen bonds with free water, yet gels based on a single biopolymer gel (BPG) or a single synthetic polymer gel (SPG) electrolytes show clear performance trade-offs, where BPGs offer biocompatibility and good interfacial regulation but lack mechanical strength and high ionic conductivity, whereas SPGs provide strong mechanical properties but poor biocompatibility and weak electrode modulation. This review examines emerging hybrid bio-synthetic gel (HB-SG) electrolytes that combine the strengths of both polymer systems, covering their design principles, four main structural types, key synergistic mechanisms, and fabrication methods. Their performance in ion transport, mechanical resilience, self-healing, temperature tolerance, and resistance to parasitic reactions is discussed alongside practical applications across flexible, extreme-environment, and harsh-condition ZIBs. Current challenges, unclear synergistic mechanisms, limited room-temperature ionic conductivity, storage instability, and industrial scalability barriers are identified, along with future directions including multiscale structural design, theoretical simulation, green manufacturing, intelligent functionalization, and biomedical applications.

KEYWORDS: gel polymer electrolytes; biopolymer; synthetic polymers; hybrid bio-synthetic gel electrolytes; zinc-ion batteries; flexible devices

Just Accepted

1. Introduction

The global transition to a low-carbon energy framework, along with the growing demand for portable electronic devices, electric mobility, and large-scale grid energy storage, has driven in-depth research into advanced electrochemical energy storage devices (EESDs) over the past few decades [1, 2]. Systems including lithium-ion batteries (LIBs), sodium-ion batteries (SIBs), zinc-ion batteries (ZIBs), metal-air batteries (MABs), metal-sulfur batteries (MSBs), supercapacitors (SCs), and photovoltaic solar cells have become fundamental technologies for modern energy infrastructure [3, 4]. Traditionally, liquid electrolytes have dominated commercial and laboratory-scale energy storage system deployments due to their room-temperature ionic conductivity (10^{-3} to 10^{-2} S cm^{-1}) and ability to form tight interfacial contacts with a variety of electrode structures [5-7]. However, the inherent drawbacks of liquid electrolytes remain a key bottleneck for long-term operational reliability and large-scale implementation. The flammability of organic solvents, spontaneous electrolyte leakage, and heterogeneous nucleation and propagation of metal dendrites collectively compromise device safety and cycle stability [8-11].

Polymer electrolytes are broadly classified into solid polymer electrolytes (SPEs) and polymer gel electrolytes (PGEs), distinguished by the presence or absence of liquid plasticizer components. SPEs represent completely solvent-free systems, where a high molecular weight polymer matrix acts as a host for dissolving and solvating ionic salts. They are widely used in all-solid-state lithium-based battery configurations, particularly lithium-sulfur (LSB) and lithium-air batteries (LABs) [12]. While SPE electrolytes offer strong mechanical integrity and enhanced operational safety, their practical applications are severely limited by slow ion transport. Typical room-temperature ionic conductivity of SPEs ranges from 10^{-8} to 10^{-5} S cm^{-1}, leading to reduced reversible specific capacity and gradual degradation of cycle performance in assembled cells [13, 14].

PGEs are positioned as an intermediate quasi-solid platform bridging liquid electrolytes and all-solid SPEs, integrating the complementary advantages of the two electrolyte classes. As a bifunctional material that can be used as both an ion conductor and an electrode separator, it has attracted increasing research interest [15]. A typical PGE architecture comprises three core components: a cross-linked polymer matrix, a dissolved electrolyte salt, and a liquid plasticizer. The polymer network physically immobilizes the bulk liquid electrolyte portion, while the incorporated plasticizer disrupts the crystallinity of the polymer chains, lowering the energy barrier for ion migration [16]. Ion conduction within

Just Accepted

PGEs primarily proceeds across the swollen gel domains and trapped liquid phases, enabling most PGE systems to achieve room-temperature ionic conductivity up to 10^{-3} S cm^{-1} [17]. This structural design effectively resolves the classic performance trade-off between the poor mechanical resilience of liquid electrolytes and the inferior ionic conductivity of all-solid electrolytes. Compounded by favorable processability and intrinsic deformability inherited from polymer backbones, PGEs are uniquely suited for the development of shape-adaptable, flexible, and wearable EESDs, cementing their status as a leading electrolyte candidate for next-generation scalable energy technologies [18, 19].

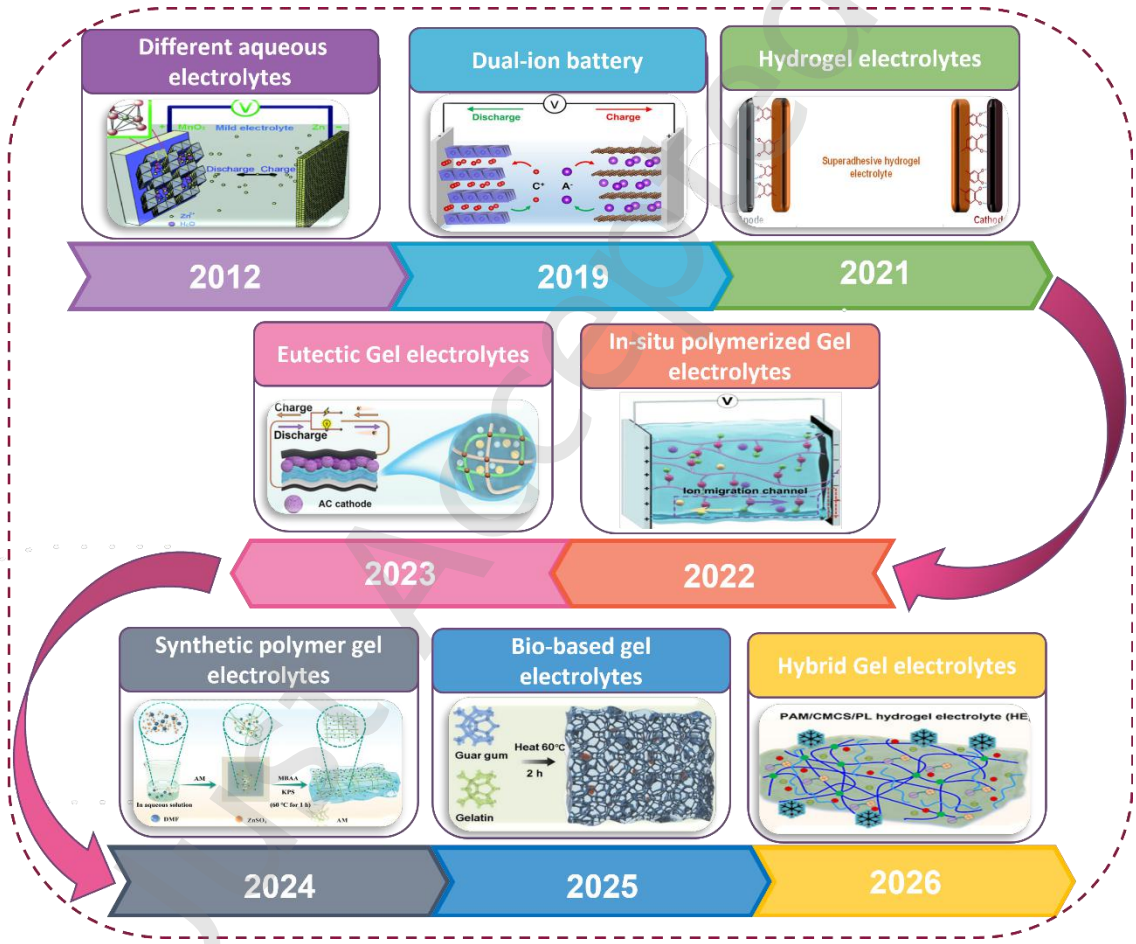


Figure 1. Evolution of polymer gel electrolyte design strategies for ZIBs, highlighting the transition from conventional polymer gels and hydrogels to advanced bio-based, functional, and hybrid gel electrolytes. Reproduced with permission [20-27].

Over the past decade, the chemistry of electrolytes for advanced aqueous and quasi-solid-state energy storage systems has advanced rapidly. Early research primarily focused on screening conventional mild aqueous electrolytes, aiming to optimize zinc-ion intercalation chemistry (2012) and expand dual-ion battery mechanisms (2019) [20, 21]. To address issues

such as liquid leakage, narrow electrochemical windows, and dendrite growth, the research focus shifted to quasi-solid-state systems, leading to the development of cross-linked hydrogel electrolytes (2021) and in-situ polymerized gel networks that improve interfacial contact (2022) [22, 23]. Subsequent advancements have resulted in non-volatile, freeze-resistant, low-melting, and deep eutectic gel formulations (2023) [24]. Recently, the field has further expanded to precisely designed synthetic polymer structures (2024), sustainable bio-based macromolecular networks derived from natural polymers (2025), and multi-network hybrid gel electrolytes designed to balance high ionic conductivity, interfacial stability, and environmental sustainability (2026), as summarized in Fig. 1 [25-27].

Traditional PGE formulations predominantly rely on synthetic polymer gel (SPG) electrolyte matrices derived from non-renewable petroleum feedstocks, including polyethylene oxide (PEO), polyvinyl alcohol (PVA), polyacrylonitrile (PAN), poly(vinylidene fluoride) (PVDF), poly(vinylidene fluoride-co-hexafluoropropylene) (PVDF-HFP), polyacrylamide (PAM), and poly(methyl methacrylate) (PMMA) [28-31]. Despite their excellent film-forming capability, tunable crosslinking behavior, and mechanical robustness, such petroleum-based SPG electrolytes present notable sustainability challenges; their non-biodegradable nature contributes to persistent white pollution, posing cumulative risks to ecological systems and human health [32]. Against the backdrop of advancing green chemistry and stringent environmental regulations, naturally derived biopolymers have emerged as a sustainable alternative for PGE fabrication [33].

Biopolymers, or natural polymers, are extracted from renewable biological sources including plants, algae and microorganisms, and are principally classified as polynucleotides, polypeptides and polysaccharides. Polysaccharides and polypeptides such as cellulose, chitosan, alginate, starch, agar and gelatin are the most widely exploited precursors for biopolymer gel (BPG) electrolytes [33]. The translational development and applied research of BPG electrolytes for EESDs have accelerated markedly, driven by their inherent advantages, natural renewability, full biodegradability, low raw material cost, facile processing routes, and non-toxic character. The sustained year-on-year growth in peer-reviewed publications on BPGs reflects the surging academic and industrial attention directed toward this material class.

Among various EESD chemicals, ZIBs stand out as a high-potential complement to mature LIB technologies. Zinc metal possesses an exceptional specific capacity of 820 mAh

Just Accepted

g^{-1} and an ultra-high volumetric specific capacity of 5846 mAh cm^{-3}, exhibits good redox potential compared to standard hydrogen electrodes, boasts abundant terrestrial zinc reserves, inherent operational safety, and low manufacturing costs [34, 35]. These characteristics make ZIB an ideal candidate for grid-level energy storage and flexible electronic applications. However, the actual commercialization of ZIBs is hindered by a series of fundamental challenges posed by traditional aqueous liquid electrolytes. The divalent Zn^{2+} ion undergoes a strong Coulomb interaction with polar water molecules, forming a stable $[Zn(H_2O)_6]^{2+}$ hydrated complex. This hydration shell imposes a large desolvation energy barrier at the electrode-electrolyte interface and hinders the extensive transport of Zn^{2+} throughout the electrolyte phase [36].

During repeated charge and discharge cycles, the continuous insertion and extraction of Zn^{2+} can cause cyclic expansion and contraction of the positive electrode lattice, resulting in sustained structural strain, ultimately leading to irreversible skeleton deformation and gradual loss of electrochemically active sites. In addition, the strong polarization effect of Zn^{2+} will generate strong electrostatic coupling with the lattice anions in the positive electrode material, distorting the original crystal structure and permanently capturing movable zinc ions, which is manifested as the gradual decay of capacity during long cycling processes [37]. The narrow electrochemical stability window (ESW) and the high chemical reactivity of aqueous media further induce harmful parasitic reactions, the hydrogen evolution reaction (HER), oxygen evolution reaction (OER), and the formation of electrochemically inert byproducts at the electrode-electrolyte interface [38]. The accumulation of these passivating substances can increase interface impedance and hinder ion diffusion pathways, while the gases produced by OER can lead to battery expansion and catastrophic device failure. In addition to interface side reactions, the polarity of water molecules also drives chemical erosion of the cathode skeleton, combined with lattice distortion and electrolyte pH fluctuations caused by cycling, accelerating the irreversible dissolution of cathode materials. On the anode side, uncontrolled growth of zinc dendrites can penetrate the separator, causing internal short circuits, while prolonged water corrosion can consume active zinc materials and electrolyte components, thereby reducing coulombic efficiency and shortening battery life [38-41]. In order to solve these problems, many mitigation strategies have been proposed, including zinc anode surface modification, electrolyte additive engineering, membrane functionalization, and gel electrolyte development. PGEs, as quasi-solid intermediates, not only retain the inherent excellent ionic

Just Accepted

conductivity and good electrode contact performance of liquid electrolytes, but also have the mechanical rigidity required to inhibit dendritic growth.

Compared with petroleum-based SPG electrolyte systems, biomass-derived BPG electrolyte systems have attracted special attention due to their ecological sustainability and complete biodegradability. Biopolymers, including sodium alginate, chitosan, cellulose, and proteins, are functionalized by introducing abundant polar groups such as hydroxyl, carbonyl, ester, aldehyde, and sulfonic acid groups [42, 43]. These functional domains effectively regulate interface chemistry, inhibit HER, and alleviate zinc anode corrosion, while also endowing the BPG electrolyte with emerging intelligent functions, including intrinsic self-healing and extreme low-temperature tolerance.[44-46] For instance, chitosan-Zn hydrogel electrolyte (HGE) achieves a tensile strength of 7.4 MPa and ionic conductivity of 71.8 mS cm^{-1}[47]. Nanocellulose-CMC systems exhibit a tensile strength of 70 MPa and ionic conductivity of 26 mS cm^{-1} [48].

Although independent BPG electrolytes have unique sustainability and functional advantages, compared with the most advanced SPG electrolytes, they generally have two key limitations: poor mechanical properties and reduced ionic conductivity [49]. At present, the optimization method of BPGs mainly relies on inorganic filler doping, physical mixing, and chemical grafting to enhance the ion transport performance, while mechanical reinforcement is still an urgent demand for manufacturing high-strength flexible batteries and implantable bioelectronic devices [50, 51]. This evolution reflects gel's broader shift from passive ion conductors to multifunctional platforms that can simultaneously regulate Zn^{2+} solvation/desolvation kinetics, stabilize the cathode electrolyte interface (CEI), and suppress material dissolution and parasitic reactions.

Herein lies the core research gap this review addresses: standalone SPG and pure BPG electrolytes each carry inherent strengths and irreconcilable drawbacks. Synthetic polymer matrices deliver exceptional mechanical toughness, controllable crosslinking, and reliable long-term structural stability, but suffer from poor environmental compatibility and limited interfacial regulatory capability. Pure biopolymers offer renewability, biodegradability, abundant reactive functional groups for interfacial modulation, and unique smart properties, yet are constrained by insufficient mechanical robustness and unsatisfactory ionic conductivity. To overcome these reciprocal limitations, Hybrid bio-synthetic gel (HB-SG) electrolyte architectures that merge biopolymer and synthetic polymer networks into a

Just Accepted

single integrated gel system emerge as a definitive next-generation electrolyte platform. HB-SG electrolytes synergistically inherit the mechanical superiority of synthetic polymers and the sustainable, functionally rich characteristics of biopolymers, while simultaneously offsetting the intrinsic defects of both single-component material classes.

To the best of our knowledge, a systematic account of HB-SG electrolytes for ZIBs has yet to be assembled in one place. Several recent reviews have covered adjacent ground: biopolymer hydrogel electrolytes for ZIB electrode-electrolyte interfaces, hydrogel polymer electrolytes for aqueous ZIBs generally, gel polymer electrolytes and electrode/electrolyte interfaces, and design/engineering strategies for polymer-hydrogel electrolytes in flexible Zn-based batteries. These reviews are organized primarily around single-component (biopolymer or synthetic) gel systems or around device-level flexibility, and do not treat HB-SGs as a distinct structural class with its own design principles and synergistic mechanisms. In contrast, this review focuses specifically on HB-SG electrolytes, organizing the field around four structural types and five coupled synergistic mechanisms in later sections, which link network chemistry to electrochemical performance, and together provide a design framework not present in the reviews above. Although GEs have advanced considerably in recent years, the rational design of HB-SG remains at an early stage, largely because the structure-property relationships that govern their behavior are still poorly understood. Therefore, it is timely to establish a coherent framework that links electrolyte design principles with their electrochemical performance. This review aims to build this framework from the basics. We first introduce the basic principles of ZIB electrolytes, elaborating on their liquid phase classification, ion transport mechanism, and key parameters for evaluating performance. On this basis, we investigated the single-component SPG and BPG electrolytes and thoroughly evaluated the advantages and limitations of each type of gel. Subsequently, this review focuses on the HB-SG electrolytes and discusses their structural design and classification, the synergistic mechanisms of mixing, the construction strategies, and the recyclability and end-of-life options. On this basis, we evaluated the performance of these mixed gels in terms of ionic conductivity, mechanical strength, wide temperature stability, self-healing ability, and their practical applications, including their compatibility with various cathode materials and applications in wearable devices, extreme temperatures, and harsh environments. Finally, we outlined the remaining challenges and identified the most promising research directions to drive the development of this field.

Just Accepted

2. Fundamental Overview: From Single-Component to Hybrid Systems

2.1 Definition and Classification of Gel Electrolytes

PGEs represent a distinctive class of quasi-solid ionic conductors that bridge the performance gap between conventional liquid electrolytes and fully solid polymer electrolytes. Modern PGEs are defined as polymeric networks crosslinked via physical interactions or covalent bonds, capable of absorbing and retaining large volumes of water or aqueous electrolyte to form stable swollen states [52, 53]. In accordance with the chemical nature of the embedded plasticizing solvent, PGE systems for EESDs and aqueous ZIBs can be systematically categorized into three primary subclasses: water-laden HGEs, organic solvent-infused gel electrolytes, and ionic liquid (IL)-based ionogel electrolytes.[54, 55] Each category possesses unique solvation environments, network characteristics, and application boundaries, which further dictate their electrochemical behavior and operational adaptability under diverse working conditions.

Among many PGEs, some stand out because of their wide application in the research of ion exchange ZIBs. This type of material is constructed by physically or chemically crosslinking hydrophilic polymer chains in an aqueous medium, ultimately forming interconnected three-dimensional (3D) network structures. This structural feature enables the PGEs to synergistically integrate the core advantages of liquid and solid electrolytes. They inherit the excellent ionic conductivity of aqueous media and the tight electrode-electrolyte interface contact, while maintaining the solid mechanical integrity brought by the crosslinked polymer framework. With this comprehensive performance, PGEs have become the preferred electrolyte candidate for the next generation of flexible batteries, wearable electronic products, and skin-attached energy devices [56-58].

From the perspective of polymeric host composition, PGEs are broadly partitioned into two fundamental families, SPGs and natural BPGs.[59] Representative synthetic polymer matrices include polyacrylamide (PAM), PVA, polyacrylic acid (PAA), and PEO. Generally, these synthesized polymers feature relatively narrow functional diversity, being functionalized with only a single dominant type of polar group along the molecular backbone.[60, 61] In contrast, biopolymers such as sodium alginate, chitosan, agarose, cellulose, xanthan gum, gelatin, and carrageenan are characterized by densely populated hydrophilic functional groups distributed across their long molecular chains [33, 62].

Just Accepted

Combined with their intrinsic eco-friendliness, widespread natural reserves, and low material cost, biopolymers have garnered escalating academic and industrial interest as sustainable alternatives to petroleum-derived synthetic polymers over the past decade. The molecular architectures and intrinsic properties of commonly adopted polymeric host materials for HGEs are summarized in Table 1.

Table 1. Commonly adopted polymeric host materials and their main properties for HGEs.[62-64]

Polymer host	Type	Typical crosslinking	Dominant groups	Main advantage	Main limitation
Polyacrylamide (PAM)	Synthetic	Chemical (MBA)	Amide (-$CONH_2$)	Strong, stretchable network	Non-renewable; few ion-regulating groups
Polyvinyl alcohol (PVA)	Synthetic	Physical (H-bond, borax); freeze-thaw	Hydroxyl (-OH)	Self-healing; good film former	Swelling; limited strength alone
Polyacrylic acid (PAA)	Synthetic	Chemical/ionic	Carboxyl (-COOH)	High water uptake; adhesive	Poor sustainability
Polyethylene oxide (PEO)	Synthetic	Physical / chemical	Ether (-O-)	Good ion solvation	Low RT conductivity; crystallizes
Cellulose	Biopolymer	Chemical/physical	Hydroxyl (-OH)	Strong, abundant, biodegradable	Needs modification to dissolve
Chitosan	Biopolymer	Ionic/covalent	Amino, hydroxyl	Interface regulation; antibacterial	pH-sensitive; brittle when dry
Sodium alginate	Biopolymer	Ionic (Zn^{2+}, Ca^{2+})	Carboxyl, hydroxyl	Fast ionic crosslinking	Weak wet strength
Gelatin	Biopolymer	Physical (triple helix)	Amide, carbonyl, amino	Biocompatible; good interface	Low strength; thermo-reversible
Xanthan gum	Biopolymer	Physical (H-bond)	Hydroxyl, carboxyl	Salt tolerance; anti-freezing	Low mechanical strength
Guar gum	Biopolymer	Physical (H-bond, borax)	Hydroxyl	Water retention; flame-resistant	Soft; swelling
Starch	Biopolymer	Physical	Hydroxyl	Cheap and	Retrogrades; weak

Just Accepted

abundant

Beyond mainstream PGE systems, organic solvent-containing gel electrolytes enable more flexible regulation of electrode-electrolyte interfacial chemistry. Organic solvent molecules can coordinate with Zn^{2+} to reduce the activity of free water, thereby suppressing the HER and mitigating zinc anode corrosion. Meanwhile, organic solvent introduction optimizes ion transport behavior at low temperatures and improves the wide-temperature adaptability of ZIBs [65, 66].

Li et al. prepared organo-HGEs by immersing freeze-dried poly(2-acrylamido-2-methylpropanesulfonic acid)/polyacrylamide hydrogel skeletons into an ethylene glycol-water binary solvent containing $ZnCl_2$/NH_4Cl. Synergistic solvation among $ZnCl_2$, ethylene glycol, and water lowers the freezing point of the electrolyte below -60 °C, and the assembled ZIBs operate stably across a broad temperature range from -30 °C to 80 °C [67]. Zhang et al. adopted a DMSO/water binary solvent system to construct organo-hydrogel electrolytes. The mixed solvent reconstructs internal hydrogen-bond networks and reduces the content of active free water molecules, simultaneously enhancing water retention and optimizing electrode-electrolyte interfaces; the corresponding batteries maintain stable performance for 3000 cycles even after 20 days of open-air exposure [68].

Ionic liquid (IL)-based ionogel electrolytes have attracted widespread attention by virtue of low vapor pressure, non-flammability, and tunable viscosity. In comparison with hydrogels and organic solvent gels, IL-based electrolytes possess a wider electrochemical stability window and superior thermal tolerance, capable of stabilizing interfacial contact between electrolytes and high-voltage cathodes and breaking the voltage limitation of conventional aqueous systems. In addition, ionic liquid environments facilitate highly reversible zinc plating/stripping and elevate the Zn^{2+} transference number. Chen et al. modified PVA PGE with 1-ethyl-3-methylimidazolium acetate ionic liquid to regulate active water molecules. Strong intermolecular interactions between PVA hydroxyl groups and the ionic liquid disrupt the hydrogen-bond network of free water, suppressing side reactions and depressing the electrolyte freezing point; the assembled Zn‖$Na_3V_2(PO_4)_3$ battery delivers a voltage plateau of 1.48 V and retains 81.3% capacity after 1600 cycles at -20 °C [69]. Liu et al. synthesized ionogel electrolytes via in-situ polymerization and crosslinking of 1-vinyl-3-ethylimidazolium dicyanamide in 1-ethyl-3-methylimidazolium dicyanamide solvent

Just Accepted

dissolved with zinc acetate. The resultant electrolyte achieves an ionic conductivity of 0.016 S cm^{-1}, and the corresponding devices operate reliably from 0 °C to 60 °C and can drive electroluminescent panels normally [70].

2.2 Basic Working Mechanism of PGEs in ZIBs

The ionic conduction path in PGEs is fundamentally different from that in pure liquid and solid electrolytes. The three-dimensional crosslinked polymer network acts as a rigid framework to fix the liquid plasticizer and dissolved zinc salt. Ion migration mainly occurs in the continuous liquid phase region captured in the swollen gel phase and along the surface of the hydrated polymer chain. For PGEs, divalent Zn^{2+} mainly exists in the form of the hydrated complex $[Zn(H_2O)_6]^{2+}$. During the charge-discharge cycle, hydrated zinc ions migrate along the interconnected water channels in the gel network, and desolvation occurs after reaching the electrode surface, releasing bare zinc ions for electroplating or embedding [71].

The polar functional groups on synthetic and biopolymer chains can form weak coordination interactions with Zn^{2+}, modulating the desolvation energy barrier and optimizing ion-transport kinetics [72]. In organic solvent and ionic-liquid-based PGEs, solvent molecules replace part or all of the water molecules to form new solvation shells around Zn^{2+}, altering ion mobility, desolvation behavior, and interfacial reaction pathways [73]. For HB-SG electrolytes, the interpenetrating dual network formed by the two types of polymers constructs hierarchical ion-transport channels, combining the fast ion conduction of liquid phases with the directional guidance of polymer chains to further improve ion migration efficiency and cation transference number. The polymeric network of PGEs forms tight physical contact with electrode surfaces, effectively isolating the zinc anode from bulk free water and inhibiting direct water-induced HER, OER, and metal corrosion. For PGE systems rich in polar functional groups, surface moieties adsorb onto the zinc anode to form a uniform protective layer, guiding homogeneous zinc nucleation and growth and suppressing the proliferation of sharp dendrites [74, 75].

At the cathode side, PGEs restrict the dissolution of transition-metal ions from cathode materials via physical confinement and intermolecular interactions, alleviating cathode structural collapse and active-material loss. For HB-SG electrolytes integrating synthetic and biopolymers, the complementary functional groups of the two components synergistically optimize interfacial chemistry; synthetic polymer segments enhance interfacial

Just Accepted

mechanical stability, while biopolymer groups (carboxylate, amino, hydroxyl) and synthetic groups (amide, sulfonate) together regulate solvation structures and suppress parasitic reactions, realizing long-term stable operation of electrode-electrolyte interfaces [63, 76-78].

2.3 Key Evaluation Parameters for PGEs

A comprehensive set of performance indicators is established to evaluate the practical applicability of PGEs for ZIBs and flexible energy devices, spanning electrochemical, mechanical, environmental, and functional dimensions [32, 79-82].

1. Ionic conductivity: the core electrochemical parameter, determining the rate capability of batteries. Measured in S cm^{-1}, high ionic conductivity ensures rapid ion migration under high current density.
2. Mechanical strength and flexibility: including tensile strength, fracture strain, compressive resistance, and bending performance. These properties guarantee structural integrity during repeated deformation and provide physical suppression of dendrite penetration.
3. Thermal stability: reflecting structural and electrochemical stability at elevated temperatures, critical for avoiding solvent volatilization, network collapse, and thermal runaway.
4. Anti-freezing performance: characterizing retention of ionic conductivity and mechanical properties under subzero conditions, which sets the low-temperature operational limit of batteries.
5. Self-healing capability: a typical smart function for flexible electronics, enabling automatic recovery of structure and electrochemical performance after mechanical damage.
6. Cycling stability: evaluating long-term performance retention during repeated charge-discharge cycles, jointly determined by network stability, interfacial durability, and side-reaction suppression.

All of the above indicators are inherently imbalanced in single-component SPG and pure BPG electrolytes. Constructing HB-SG electrolyte systems is an effective strategy to break

Just Accepted

through these performance trade-offs and realize comprehensive optimization of all key parameters.

3. Single Component Gel Electrolytes

3.1 Synthetic Polymer Gel Electrolytes

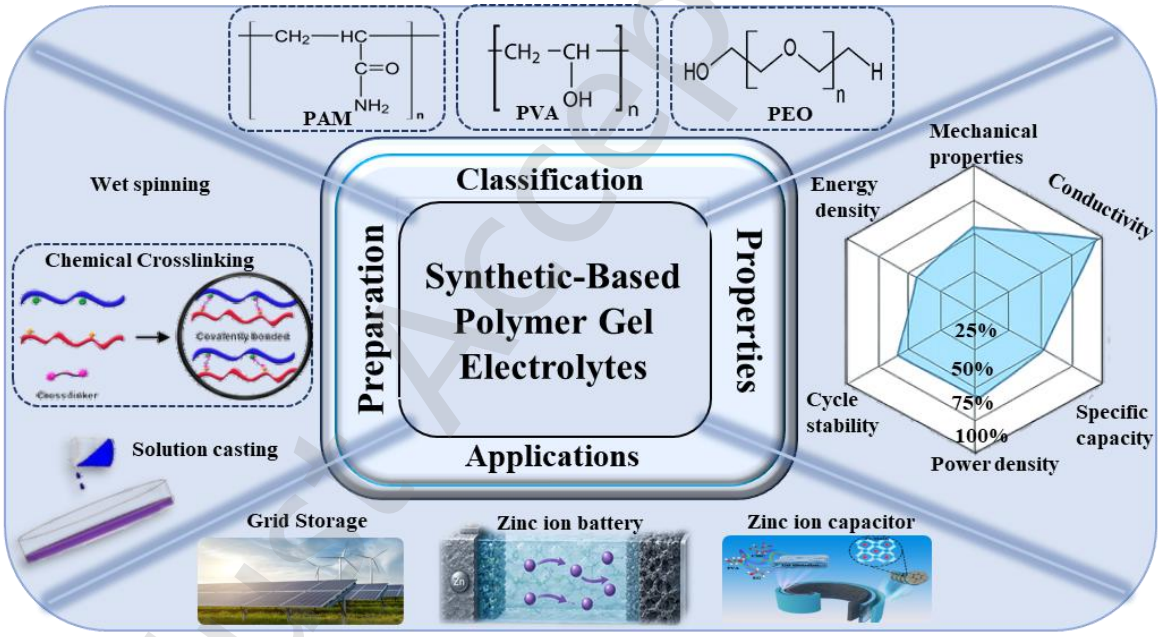


Figure 2. An overview of synthetic-based polymer gel electrolyte classifications for zinc-ion batteries. Representative synthetic polymer hosts are shown with their repeat-unit structures, alongside common fabrication routes, a qualitative property profile, and representative device applications [83-85].

Synthetic polymers are produced by the controlled polymerization of well-defined monomers and offer easy accessibility, structural stability, and superior mechanical performance. Fig. 2 shows that synthetic polymers such as PAM, PVA, PAA, and PEO are typically processed by wet spinning, chemical crosslinking, or solution casting into gel electrolytes with strong mechanical properties and high conductivity. Their backbones are

Just Accepted

dominated by flexible C-C and C-O-C single bonds with few rigid segments, which lowers the steric barrier to segmental motion and allows the chains to rearrange and entangle readily during gelation. Dense chain entanglement and tunable crosslinking give these gels high elastic deformability and mechanical properties that can be adjusted through the choice of monomer, crosslinker, and network density [86, 87]. Many common hosts, PVA, PAA, PAM, and PEO, also carry hydrophilic groups that form intra- and inter-chain hydrogen bonds, reinforcing the network and helping immobilize water within it [88]. Because polymerization parameters such as monomer ratio and reaction conditions can be finely controlled, synthetic hosts are also highly amenable to functional modification. Below, the four most widely used synthetic hosts for zinc-ion gel electrolytes are discussed in turn.

3.1.1 Polyacrylamide (PAM)

PAM is one of the most widely used synthetic matrices for PGEs. Its abundant amide ($-CONH_2$) groups adsorb and retain large amounts of water, building continuous ion-transport channels within the gel [89]. Acrylamide monomer is typically polymerized with N, N′-methylenebis(acrylamide) (MBA) as the crosslinker; when aluminium polycations are introduced as crosslinkers, the radicals generated can also react with residual monomer at the electrode surface, driving in-situ formation and self-repair of the cathode electrolyte interphase and suppressing cathode hydrolysis under high potential [89, 90]. Li et al. used crosslinked PAM gel electrolytes to build waterproof, tailorable yarn-type ZIBs; the optimized electrolyte delivered an ionic conductivity of 17.3 mS cm^{-1}, and the flexible cell achieved a specific capacity of 302.1 mAh g^{-1}, a volumetric energy density of 53.8 mWh cm^{-3}, and 98.5% capacity retention after 500 cycles at 2 A g^{-1} [63].

3.1.2 Polyvinyl Alcohol (PVA)

PVA is a low-cost, non-toxic host with strong hydrophilicity and good film-forming ability. Extensive hydrogen bonding between PVA chains underpins its intrinsic self-healing behavior, and its mechanical strength is usually developed through freeze-thaw or borax crosslinking rather than the pristine polymer alone [91, 92]. Huang et al. developed PVA/$Zn(CF_3SO_3)_2$ HGEs with an ionic conductivity of 12.6 mS cm^{-1} that fully recovered their electrochemical function after repeated cutting and healing, owing to reversible reconstruction of intermolecular hydrogen bonds [93]. PVA has also been employed as a PGE in Zn//D-MoS_2-O batteries, owing to its excellent flexibility and efficient ion transport; the PVA-based PGEs enabled the fabrication of a flexible quasi-solid-state battery with

Just Accepted

promising electrochemical performance. The device exhibited a high ionic conductivity of 9.76 mS cm^{-1} and an operating voltage of 2.2 V. In addition, it delivered a specific capacity of 215.0 mAh g^{-1} at a current density of 0.1 A g^{-1}, demonstrating the suitability of PVA PGEs for flexible zinc-ion battery applications [94].

3.1.3 Polyacrylic Acid (PAA)

PAA carries dense carboxyl (-COOH) groups and is widely used as a battery binder through carboxyl-derived hydrogen bonding; electrostatic interaction between carboxylate anions and metal cations further reinforces the network. Ouyang et al. introduced ionized PAA chains to reconstruct the Zn^{2+} solvation structure and form in-situ adsorption layers on the zinc anode, accelerating Zn^{2+} transport kinetics while suppressing anode side reactions and cathode dissolution [95]. A fiber-shaped electrode using a double-crosslinked PAA PGE containing 2 M $ZnSO_4$ electrolyte was reported. The primary network is formed through permanent covalent crosslinking. Meanwhile, a secondary network based on reversible hydrogen bonding between the carboxyl groups of the PAA chains effectively dissipates mechanical stress during deformation. As a result, the PGE exhibits exceptional stretchability, sustaining strains of up to 2500% with a tensile stress of 250.1 kPa. In addition, the abundant carboxyl groups facilitate the retention of water molecules and Zn^{2+} ions, enabling efficient ion transport. Consequently, the PGE achieves a high ionic conductivity of 21.7 mS cm^{-1}, while maintaining 19.8 mS cm^{-1} even under 250% tensile strain [96].

3.1.4 Polyethylene Oxide (PEO)

PEO is one of the most extensively studied polymer hosts for electrolyte applications because of its ether oxygen-rich backbone, which provides multiple coordination sites for metal cations, while its flexible molecular chains promote efficient ion migration. In addition to excellent ion transport performance, PEO also has good biocompatibility, excellent hydrophilicity, high viscosity, and ideal mechanical flexibility. The presence of terminal hydroxyl groups enables them to form hydrogen bonds with ether oxygen atoms, further enhancing their multifunctionality in a wide range of electrochemical and material applications [97]. Zou et al. doped zinc-rich ionic conductors into PEO gels to lower matrix crystallinity, simultaneously improving ionic conductivity and mechanical performance; the optimized PEO-based electrolyte reached an ionic conductivity of 1.32 x 10^{-3} S cm^{-1} with a Zn^{2+} transference number of 0.86 [30]. However, pure PEO electrolytes still have some inherent defects, including limited ionic conductivity at room temperature due to their high

Just Accepted

crystallinity, poor compatibility with electrode interfaces, and insufficient chemical stability [98]. These shortcomings restrict their practical implementation in high-energy-density battery technologies.

3.1.5 Advantages and Drawbacks of Synthetic Polymer Gels

Taken together, synthetic hosts offer clear strengths: flexible backbones and dense chain entanglement give strong, stretchable networks; hydrophilic groups support hydrogen bonding and water retention; polymerization and post-modification allow precise control of molecular weight, crosslink density, and functionality; and good solution processability enables uniform, large-area films by casting or electrospinning, compatible with coin, pouch, and flexible cells [33, 90].

These merits are offset by several intrinsic limitations that restrict long-cycle use in ZIBs. Most synthetic hosts are petroleum-derived and non-biodegradable, conflicting with the sustainability rationale of ZIBs. Their gels adapt poorly to temperature extremes, free water freezes, and chain mobility falls at low temperature, while solvent volatilizes and networks shrink at high temperature. Weak polymer-water interactions also make them prone to dehydration during cycling or open storage, degrading the ion-transport network. Most critically, a single dominant functional-group type gives limited capacity to regulate the Zn^{2+} solvation structure, suppress dendrites, or inhibit water-induced HER/OER and anode corrosion; this weak interfacial regulation is the principal shortcoming of single-component SPG electrolytes.

This limitation is structural rather than incidental. Effective Zn^{2+} desolvation and anion or dendrite control benefit from a graded coordination environment: sites that bind Zn^{2+} more strongly than water and displace part of its hydration shell, together with sites that interact with anions or guide deposition. A homopolymer carries one repeating group and therefore one binding strength and geometry. The PAM amide does enter the Zn^{2+} first shell, but it binds more weakly than carboxylate in the same system (-0.11 vs -0.19 eV), and a PAM gel gave a Zn^{2+} transference number of only 0.47 [78]. Single-group hosts can still reshape the shell when the group binds strongly, as ionized PAA does [95], but binding that is too strong raises viscosity and lowers Zn^{2+} diffusivity [99]. PEO adds a second limit: Zn^{2+} transport occurs mainly through segmental motion in amorphous domains, so crystalline regions obstruct hopping pathways and keep room-temperature conductivity low despite reasonable solvation ability [30, 94, 95]. Multi-group hosts such as biopolymers (hydroxyl,

Just Accepted

carboxylate, amino) can supply several binding chemistries on one chain, but the effect depends on group type, density, and ionization state rather than on biological origin [30, 97, 98]. The biopolymer systems (e.g., chitosan's amino/hydroxyl pairing, carboxylate/hydroxyl pairing) present two or more distinct donor-group chemistries on the same chain, which is why they support achieving interfacial regulation that single-functional-group hosts cannot achieve [100, 101].

3.2 Biopolymer Gel Electrolytes

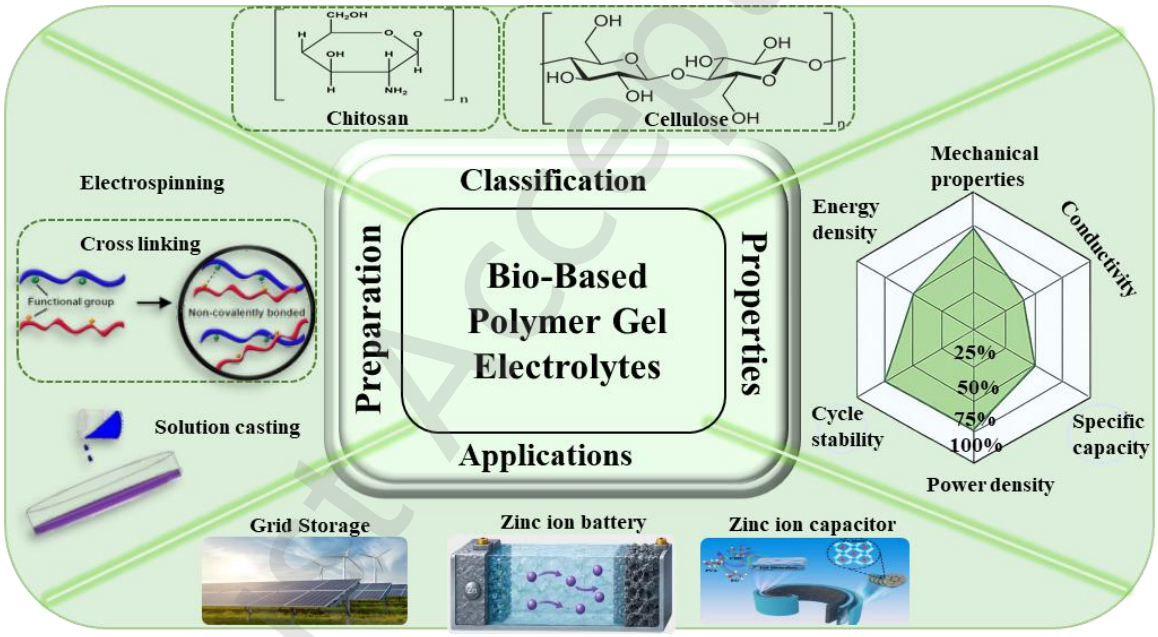


Figure 3. An overview of bio-based polymer gel electrolyte classifications for zinc-ion batteries. Representative biopolymer sources are shown with their structures, alongside common fabrication routes, a qualitative property profile, and representative device applications [83-85].

Natural biopolymers are extracted from renewable sources such as plants, algae and microorganisms, and their long chains carry densely populated polar groups hydroxyl, carboxyl and amino, which build stable three-dimensional networks through hydrogen bonding, ionic interaction and van der Waals forces. As shown in Fig. 3, biopolymers including chitosan, cellulose, alginate and proteins are processed by electrospinning or non-

Just Accepted

covalent crosslinking into gel electrolytes that offer a more balanced, renewable-derived property profile. Combined with renewability, biodegradability, low cost, and non-toxicity, these features make biopolymers attractive hosts for zinc-ion gel electrolytes. Sodium alginate, chitosan and cellulose are the most widely used, and their abundant reactive groups also provide sites for crosslinking and chemical modification that tune water content, mechanical properties and interfacial behavior.

3.2.1 Chitosan

Chitosan is a biodegradable, semi-crystalline polysaccharide of glucosamine and N-acetylglucosamine units, rich in hydroxyl and amino groups that give strong adsorption, good desolvation ability, and proton-storage capacity.[102] Pure chitosan electrolytes suffer from relatively low ionic conductivity, so modification is common; supramolecular complexation with metal ions (Li^+ , Ag^+) yields thermally stable, mouldable PGEs, carboxylated chitosan forms non-covalent gel films using HCl as a crosslinker with usable performance in all-solid-state ZIBs, and blending with PAM builds dual-network gels combining high stretchability, high conductivity, and wide temperature tolerance [103]. Wu et al. developed zinc-coordinated chitosan electrolytes with strong mechanical strength, high Zn^{2+} conductivity, and good water retention; the electrolyte induced uniform hexagonal zinc-platelet deposition, achieving 99.7% coulombic efficiency and stable cycling over 1000 cycles at 50 mA cm^{-2} [47].

3.2.2 Cellulose and Its Derivatives

Cellulose and its derivatives are ideal biopolymer hosts by virtue of low cost, intrinsic mechanical strength, flexibility, and mild-condition biodegradability. Microcrystalline cellulose offers high crystallinity and tensile strength, while carboxymethyl cellulose (CMC) can act as both a gelling agent and matrix and can be crosslinked with citric acid to form self-healing gels. However, the presence of intermolecular hydrogen bonds makes cellulose difficult to process and only soluble in specific solutions [104]. Cellulose nanofibers (CNF) are frequently blended with PAM or other polymers to build interpenetrating double-network PGEs, in which added ions strengthen chain water interactions to suppress ice formation and evaporation, giving high conductivity and stretchability at low temperature [105]. A Zn^{2+}-coordinated carboxylated cellulose nanofibril/xanthan gum (Zn-CCNF@XG) solid-state electrolyte was developed to improve ion transport in zinc-ion batteries. The coordinated carboxyl groups and engineered ion-conduction channels facilitate Zn^{2+} migration, resulting

Just Accepted

in a high ionic conductivity of 1.17 × 10^{-4} S cm^{-1} and a Zn^{2+} transference number of 0.78. When assembled with a Zn||$NaV_3O_8 \cdot 1.5H_2O$ full cell, the electrolyte delivered excellent cycling stability, retaining 83.46% of its capacity with a 99.99% coulombic efficiency after 3000 cycles at 1 A g^{-1} [106].

3.2.3 Alginate

Alginate is a natural polysaccharide that is commonly extracted from brown algae. Alginate, an anionic polysaccharide from brown seaweed, is a promising host owing to abundant hydroxyl and carboxyl groups. Alginate-based PGEs have attracted significant attention for electrochemical applications because of their excellent hydrophilicity, biocompatibility, and low cost. While alginic acid is poorly soluble in water, sodium alginate (SA) readily dissolves in aqueous media, making it a preferred precursor for PGE fabrication [107]. It can serve simultaneously as electrolyte, separator, and binder to build additive-free all-alginate ZIBs with high volumetric capacity and stable cycling. Sodium Alginate is commonly combined with PAM to form dual-crosslinked interpenetrating networks, where covalently crosslinked PAM is entangled with dispersed SA chains; when crosslinked by Al^{3+}, the Al-alginate/PAM gel shows reversible deformation and efficient energy dissipation, markedly improving mechanical durability. Zhang et al. prepared tannic-acid-modified sodium alginate (TA-SA) gel electrolytes with an ionic conductivity of 24.2 mS cm^{-1} and a Zn^{2+} transference number of 0.74; the ion-confinement effect suppressed dendrite growth and water-induced side reactions and alleviated $NH_4V_4O_{10}$ cathode dissolution, delivering 238.6 mAh g^{-1} and 94.5% retention after 900 cycles at 2 A g^{-1} [101].

3.2.4 Other Biopolymers

Several further biopolymers have been explored as zinc-ion hosts, including agarose, gelatin, lignin, starch, soy protein, and gums such as carrageenan [108]. Agarose forms porous physical gels with abundant ion channels but is mechanically weak on its own, so agarose/PAM double networks are used to raise strength and recoverability [109]. Gelatin offers excellent biocompatibility and water solubility but insufficient strength and thermal stability, which double-network organohydrogels improve alongside anti-freezing and anti-drying behavior [110]. Xanthan gum contributes structural uniformity, high viscosity, and water retention; carrageenan combines high ionic conductivity with environmental friendliness, and carrageenan/PAM dual-network gels show robust mechanical and electrochemical performance for flexible ZIBs [111, 112]. Lignin-based gels formed by

Just Accepted

chemical crosslinking and acid treatment give hybrid dual-crosslinked networks with high strength, shape recovery, and conductivity [113].

3.2.5 Advantages and Drawbacks of Biopolymer Gel Electrolytes

Biopolymer hosts bring complementary strengths to zinc-ion PGEs. Their dense hydrophilic groups build stable networks and provide numerous sites for modulating Zn^{2+} transport and interfacial chemistry. Strong chain water hydrogen bonding restricts ice formation, giving good anti-freezing behavior and maintaining conductivity and flexibility below 0 °C. Their natural origin confers biocompatibility and low immunogenicity, enabling wearable and implantable devices, while hydrolysable backbones make them biodegradable at a tunable rate, though this same degradability must be balanced against the need for long-term operational stability. High molecular weight also promotes chain entanglement that helps maintain network integrity during assembly and cycling [33, 45, 114].

Their main limitation lies in their mechanical properties; that is, single-component BPG electrolytes usually have low tensile strength, limited fracture toughness, and a narrow deformation range, which limits their application in high-strength flexible implantable zinc ion batteries. Unlike the permanent covalent crosslinks of synthetic hosts, most biopolymer networks rely on physical interactions, hydrogen bonding (cellulose, chitosan), ionic crosslinking (alginate-Ca^{2+}/Zn^{2+}), or helix formation (gelatin) that are inherently dynamic and reversible. Under mechanical load, these bonds continuously dissociate and reform rather than bearing stress permanently, so the network dissipates energy effectively but cannot sustain high stress without creep or rupture. This is the direct cause of the low tensile strength and poor wet-state stability summarized in Table 1 (alginate's weak wet strength, chitosan's brittleness when dry)[115]. Compared with the optimized SPG electrolytes, their ionic conductivity is often lower and more unstable. The modification methods include ion crosslinking or functionalization of chitosan, breaking the hydrogen bonds of cellulose and reducing its crystallinity, and constructing a three-dimensional skeleton of alginate. The same physical crosslink dependence also explains the batch-to-batch variability associated with natural sources, because crosslink density depends on chain length, molecular weight, and purity properties that vary with biological origin and extraction method. It is inherently harder to standardize than a synthetic network built on a fixed crosslinker-to-monomer ratio. However, the core solution is to enhance interchain crosslinking, and interpenetrating networks are the most effective way to achieve this [116]. PAM is the preferred material for achieving this goal, as it has good miscibility with biopolymers, a robust mechanical structure,

Just Accepted

and amide groups that can fix water molecules and provide continuous ion channels. It is this limitation and the resulting interpenetrating network solution that prompted us to discuss the HB-SGs in the next section.

4. Hybrid Bio-Synthetic Gel electrolytes

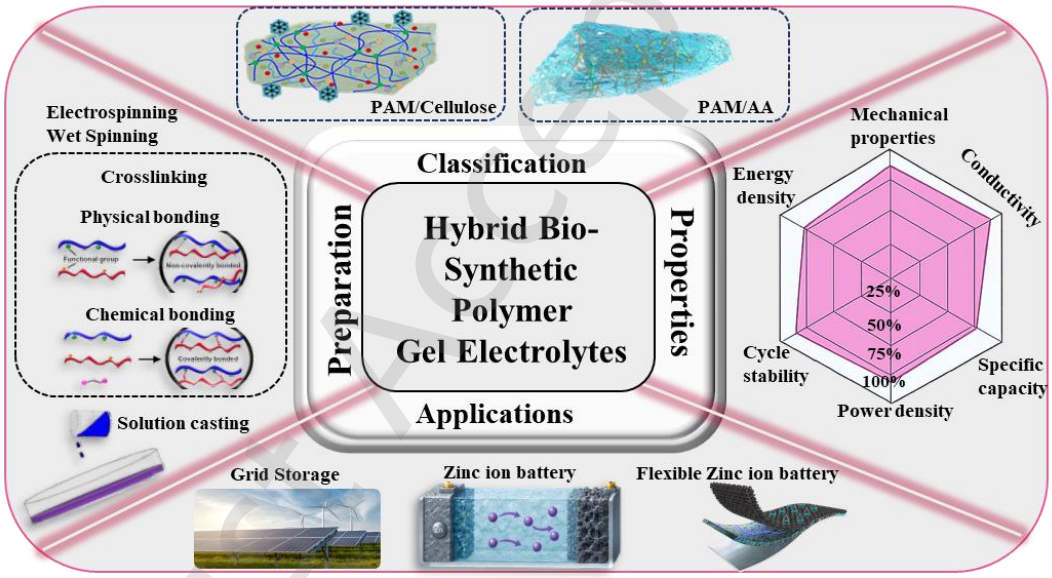


Figure 4. An overview of hybrid bio-synthetic polymer gel electrolyte classifications for zinc-ion batteries. Representative hybrid systems (PAM/cellulose, PAM/acrylic acid) are shown alongside the two principal crosslinking strategies, a qualitative property profile, and representative applications [83-85].

The separate application of pure SPG and BPG electrolytes has been limited by performance trade-offs for a long time, which hinders their practical application in solid ESSDs, especially ZIBs. Synthetic polymer matrices such as PAM and PVA have stable covalent crosslinking structures, providing strong mechanical rigidity, excellent film-forming properties, and long-term structural durability. However, these petroleum-derived materials have drawbacks such as non-biodegradability, continuous dehydration during cycling, and

Just Accepted

limited ability to regulate electrode interface behavior (including zinc dendrite growth and parasitic side reactions). On the contrary, natural biopolymers represented by cellulose, chitosan, sodium alginate (SA), gelatin, and carrageenan are rich in polar functional groups (hydroxyl, carboxyl, and amino), inherent biodegradability, excellent biocompatibility, and significant low-temperature resistance, which enable them to effectively regulate zinc ion migration and inhibit anodic corrosion. However, their network structure is mainly maintained by weak non-covalent interactions, resulting in poor mechanical strength, susceptibility to structural collapse, relatively low ionic conductivity, and poor batch consistency [117].

Against this technical backdrop, the rational design of HB-SG electrolytes emerged as a pivotal research direction. As shown in Fig. 4, HB-SG electrolytes combine physically and chemically crosslinked biopolymer-synthetic networks (e.g., PAM/cellulose, PAM/AA), coordinating Zn^{2+} directly within the network and extending the usable temperature range to as wide as -70 °C to 100 °C. The core design paradigm integrates synthetic polymer and natural biopolymer components within a unified network architecture to mutually reinforce favorable attributes and mitigate the intrinsic deficiencies of each single-component system. Rather than a trivial physical admixture, the targeted construction of multi-component interpenetrating, or hybrid crosslinked networks couples the mechanical superiority of synthetic polymers with the interfacial regulation, eco-friendliness, and extreme-temperature adaptability of biopolymers. This design philosophy helps overcome the performance bottlenecks of conventional single-component gel electrolytes and provides a framework for developing high-performance, multifunctional gel materials for next-generation energy storage systems [118-121].

4.1 Structural Design and Classification of HB-SG electrolytes

HB-SG electrolytes are classified into four architectures according to how the synthetic and biopolymer components are organized, bonded, and reinforced. Because these descriptors capture different structural features, one electrolyte may show characteristics of more than one category, so two questions are best separated. The first is how the components are arranged: as two discrete, interpenetrating networks (dual network) or as a single, molecularly homogeneous phase (blended composite) [122]. The second is what holds them together. Li et al. divide GPE crosslinking into physical (entanglement, ionic, and electrostatic) and chemical (covalent) routes, the latter giving a more stable, higher-strength network [63]. These two choices are independent. A dual-network electrolyte, for instance,

Just Accepted

commonly pairs a covalently crosslinked synthetic network with a second network held together only by ionic or hydrogen-bond crosslinking [123], and a blended composite can gel through hydrogen bonding alone. Dual-network and blended electrolytes may therefore contain supramolecular interactions without being classed as supramolecular systems. We reserve that term for electrolytes in which reversible, dynamic non-covalent interactions (host-guest recognition, metal-ion coordination, or hydrogen-bond networks) are the primary engineered feature, responsible for adaptive, self-healing, or environment-responsive behavior [124], rather than an incidental result of using a biopolymer. Organic–inorganic reinforcement, finally, refers to the presence of inorganic fillers and can be applied to any of the three architectures.

Just Accepted

4.1.1 Dual-Network HB-SG electrolytes

Dual-network (DN) architectures are the most widely explored hybrid configuration, consisting of two mutually interpenetrated yet structurally independent polymer networks without phase segregation. Typically, the first network is constructed from rigid synthetic polymers (e.g., PAM, HPAAm) to bear mechanical loads, while the secondary network is composed of flexible natural biopolymers (agarose, carrageenan, cellulose) that dissipate strain energy through reversible intermolecular interactions. This topological design balances stiffness with ductility and has been widely adopted for flexible and durable zinc-ion batteries [125, 126]. Mechanistically, DN architectures are typically built in two stages. A covalently crosslinked synthetic network is formed first, for example by UV-initiated radical polymerization of a vinyl monomer with a chemical crosslinker. The biopolymer, introduced either in the precursor or afterwards, is then crosslinked in situ by physical interactions such as ionic coordination, without covalent bonding to the first network. For example, Zeng et al. first UV-polymerized N-methylolacrylamide with a chemical crosslinker to build a covalent PNMA scaffold, then immersed it in $Zn(ClO_4)_2$ solution so that Zn^{2+} carboxylate ionic coordination formed a second, sodium-alginate network in situ, the resulting PNMA/SA dual-network electrolyte reached a tensile strength of 838 kPa and an ionic conductivity of 33.1 mS cm^{-1} [123].

4.1.2 Blended Composite HB-SG electrolytes

This category is fabricated via molecular-level homogenization of synthetic polymer chains and biopolymer chains in aqueous media, followed by gelation driven by hydrogen bonding, electrostatic attraction, or ionic crosslinking. Unlike dual-network systems with discrete network phases, blended hybrid gels form a homogeneous single-phase network. The component ratio can be flexibly modulated to tailor overall performance, giving facile fabrication and good scalability for laboratory research and preliminary industrial exploration [60]. Concretely, Sun et al. dissolved PVA and gelatin directly into a 10 M $ZnCl_2$ water-in-salt solution and stirred at 60 °C for 3 h to achieve molecular level mixing, then cast the homogeneous solution into a mold and allowed it to cool gradually to room temperature; gelation proceeded purely through physical hydrogen bonding interactions among PVA, gelatin, and the Zn^{2+} bound water, without any covalent crosslinker, yielding a compositionally uniform hydrogel electrolyte with an ionic conductivity of 110.2 mS cm^{-1} and 96.2% capacity retention after 8000 cycles [127].

4.1.3 Supramolecular HB-SG electrolytes

Unlike dual-network and blended composite systems, where non-covalent interactions typically arise as a byproduct of using a biopolymer component, supramolecular HB-SG electrolytes deliberately exploit reversible, dynamic non-covalent interactions host guest recognition, metal-ion coordination, and hydrogen-bond networks as the primary design mechanism for adaptive ion transport, self-healing, or stimulus-responsive behavior, distinguishing them from dual-network and blended composite systems in which non-covalent interactions are present but not the main engineered function[128]. A representative example is the PAMCD gel electrolyte, which integrates a PAM network with β-cyclodextrin (β-CD, a starch-derived cyclic oligosaccharide) in the presence of chaotropic ClO_4^- anions. Here, β-CD's host-guest interaction with $ClO4^-$ restricts its migration, while the chaotropic anions themselves disrupt the intrinsic hydrogen-bond network of water, increasing the proportion of weak hydrogen bonds and promoting Zn^{2+}-ClO_4^- decoupling; the amide groups on the PAM chains further anchor water molecules to destabilize residual ordered water structure. These synergistic, reversible interactions (rather than a fixed covalent scaffold) are the system's primary functional design target; at high salt concentration, they simultaneously depress the electrolyte's freezing point to -80 ºC, raise ion mobility, and impart high mechanical ductility (707% elongation). The resulting electrolyte sustained Zn||Zn symmetric cells for 5290 h at 0.5 mA cm^{-2} and 1960 h at 5 mA cm^{-2}, and enabled Zn||polyaniline full cells to retain 100.8 mAh g^{-1} after 7600 cycles at -40 ºC [124].

Just Accepted

4.1.4 Organic-Inorganic Reinforced HB-SG electrolytes

Organic–inorganic reinforced HB-SG electrolytes incorporate a deliberately added inorganic nanophase, such as silica, clay, or MXene, into a biopolymer synthetic polymer gel. The polymer network remains the continuous skeleton, while the filler provides mechanical reinforcement and additional control over water structure and Zn^{2+} transport. The filler is typically dispersed in the precursor before gelation so that its surface groups interact with the chains as the network forms [129]. For example, Wang et al. dispersed TEMPO-oxidized cellulose nanofibers (CNF) and nano SiO_2 in an ethylene glycol (EG)/water mixture, dissolved PVA in the suspension in 2 M $ZnCl_2$ at 90 ºC, and gelled the mixture by freeze-thaw cycling at -20 ºC. The cycling forms PVA microcrystalline domains that act as physical crosslinks, and the hydroxyl rich SiO_2 and CNF hydrogen-bond with PVA chains and hinder crack propagation. The resulting PSC hydrogel reached 6.1 MPa and 528% elongation (2.2 MPa and 317% for PVA alone), with an optimal CNF to PVA ratio of 5 wt%. EG disrupts the hydrogen-bond network of water and reconfigures the Zn^{2+} solvation sheath, so no ice formed down to -30 ºC. The gel retained a conductivity of 42 mS cm^{-1} at -20 ºC, and Zn||V_2O_5 cells delivered 223 to 103 mAh g^{-1} from 80 to −20 ºC [130].

4.2 Synergistic Mechanisms in HB-SG electrolyte Networks

The performance superiority of HB-SG electrolytes does not arise from simple property averaging; it emerges from several coupled, mutually reinforcing mechanisms operating at the molecular, network, and interfacial scales. Five mechanisms are examined below, each linked to representative quantified evidence.

Just Accepted

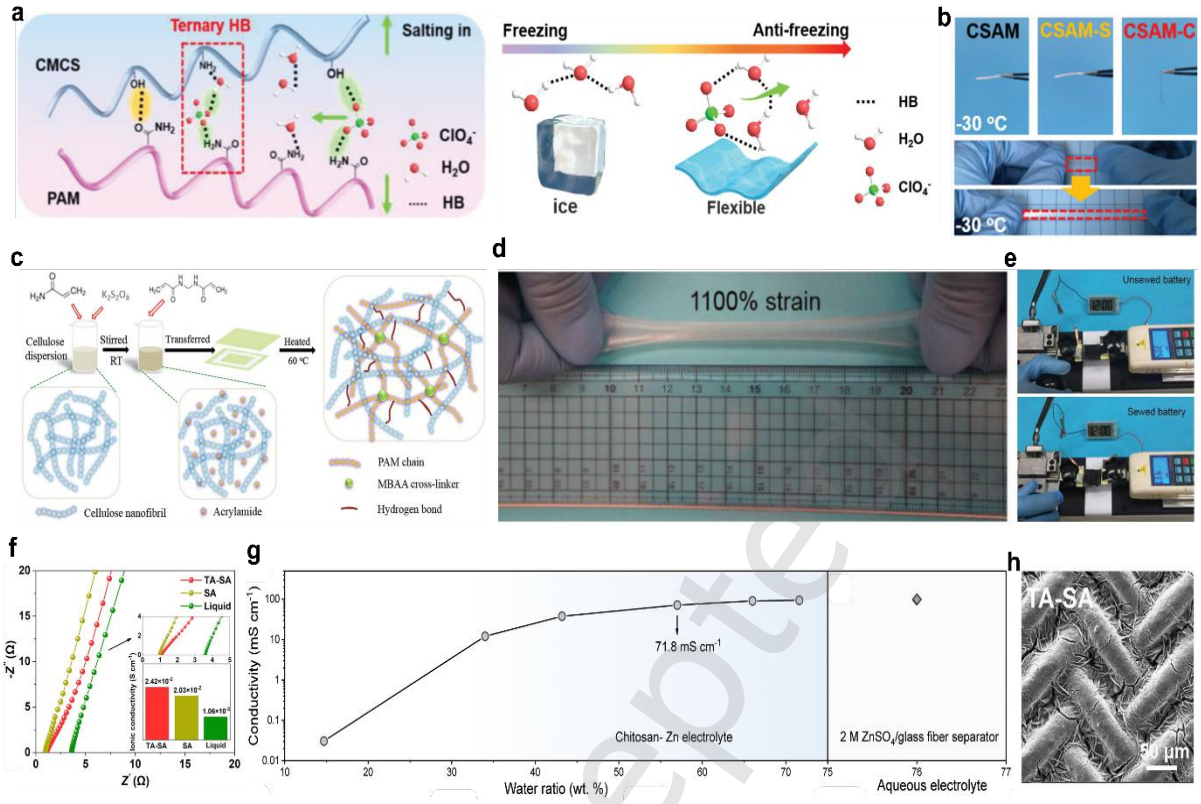


Figure 5. Structural design, mechanical robustness, and electrochemical performance of representative HB-SG electrolytes for flexible zinc-ion batteries. (a) Schematic of the ternary hydrogen-bond (HB) network formed between CMCS, PAM, ClO_4^-, and H_2O, illustrating the salting-in effect and the freezing/anti-freezing transition of water molecules within the gel. Reproduced with permission. (b) Photographs of CSAM, CSAM-S, and CSAM-C hydrogels remaining flexible and bendable at -30 °C. Reproduced with permission [66]. (c) Fabrication route of the cellulose nanofibril/PAM hydrogel via free-radical polymerization at 60 °C, and the resulting crosslinked network schematic. Reproduced with permission. (d) Photograph demonstrating the gel's stretchability, withstanding 1100% strain. Reproduced with permission. (e) Electrochemical performance comparison of an unsewed versus sewed flexible battery. Reproduced with permission [131]. (f) Nyquist plots of the TA-SA, SA, and liquid electrolytes, with the inset showing their corresponding ionic conductivities. Reproduced with permission [101]. (g) Ionic conductivity of the chitosan-Zn HB-SG electrolytes as a function of water content, reaching a maximum of 71.8 mS cm^{-1}. Reproduced with permission. (h) Cross-sectional SEM image of the TA-SA hydrogel showing its porous network morphology. Reproduced with permission [101].

4.2.1 Molecular Hydrogen-Bond Synergy

Just Accepted

Synthetic hosts (PAM, PVA) and biopolymers (chitosan, SA, gelatin) both carry dense hydroxyl, amide, and carboxyl groups, but with different donor/acceptor character. When the two are combined, a large population of inter-chain hydrogen bonds forms across the synthetic-biopolymer interface in addition to the intra-chain bonds present in each component alone. These inter-network bonds act as reversible physical crosslinks superimposed on the covalent junctions, raising the effective crosslink density and network connectivity well beyond that of either single-component gel. Because hydrogen bonds break and reform dynamically, they also serve as sacrificial linkages that dissipate energy without permanent network damage, which is the molecular origin of the toughness gain. Fig. 5(a) shows a representative example of carboxymethyl-chitosan(CMCS)/PAM (CSAM) dual-network gel, in which ClO_4^-, water, and polymer chains form ternary hydrogen bonds under the Hofmeister effect. The resulting network, even at -30 °C, delivered an ionic conductivity of 7.80 mS cm^{-1} and retained flexibility (fig. 5(b)). DFT on the CSAM system gives a binding energy of -58.06 kJ mol^{-1} for PAM/water against -21.35 kJ mol^{-1} for water/water, and -97.16 kJ mol^{-1} for PAM-ClO_4^-, so both the polymer and the chaotropic anion compete with water/water hydrogen bonding. Low-field NMR shows that nearly all free water is converted to bound water, and the gel retains 80.1% of its water after 48 h, against 52.6% in $ZnSO_4$ and 34.8% without salt, $t_{(Zn^{2+})}$ is 0.76 against 0.39 for the liquid $Zn(ClO_4)_2$ electrolyte. Beyond structural reinforcement, this hydrogen-bond network reorganizes the population of free versus bound water, by immobilizing free water molecules, it lowers water activity, which narrows the fraction of electrochemically active water and suppresses the water-induced HER/OER that erodes coulombic efficiency in aqueous cells [66].

Just Accepted

4.2.2 Mechanical Toughness Complementation

When two networks fail in opposite modes, combining them converts each weakness into a strength. The rigid, covalently crosslinked synthetic network bears the primary tensile and compressive load and provides shape retention, while the physically crosslinked biopolymer network acts as a sacrificial, energy-dissipating phase. Its ionic and hydrogen-bond junctions rupture preferentially under stress, blunting crack propagation before the load-bearing network fractures, then reform to restore integrity. This division of labor overcomes both the brittleness of pure BPG electrolytes and the limited ductility of pure SPG

electrolytes. The effect is large and well-documented [132-134]. As shown in Fig. 5(c-e), the cellulose-nanofibril/PAM dual-network gel is formed by polymerizing acrylamide through a pre-existing cellulose nanofibril framework, where covalent PAM crosslinks and inter-chain hydrogen bonds interweave the two networks. In this gel, the preformed nanofibril network raises the tensile strength from 38 kPa for PAM to 158 kPa, enlarges the pores from 20-40 μm to 60-180 μm, and raises σ from 16.9 to 22.8 mS cm^{-1}, consistent with the nanofibrils holding open large channels while hydrogen bonds and entanglement with PAM reinforce the walls. This design lets the gel stretch without rupture, as the covalent network bears the load while the fibrils and reversible hydrogen bonds dissipate energy. Critically, a sewn cell pierced and stitched with thread still powers a digital display as well as the unsewed one, confirming that ionic continuity and interfacial contact survive severe mechanical damage, ideal for wearable, textile-integrated zinc-ion batteries [131].

4.2.3 Interface Modulation and Ion-Transport Regulation

Both components can reshape the Zn^{2+} solvation shell, and their roles are complementary rather than interchangeable. In dilute aqueous electrolytes, Zn^{2+} is coordinated by six water molecules, and a polymer group that binds Zn^{2+} more strongly than water competes for these sites and releases water from the shell [99]. In a CS/PAM electrolyte, the DFT binding energy of PAM (-1.24 eV) exceeds that of water (-0.64 eV), and PAM enters the Zn^{2+} first shell [135], while a cationic poly(acrylamidopropyl trimethylammonium) hydrogel lowers the Zn^{2+} water coordination number from 3.88 to 3.05 by electrostatic repulsion rather than coordination [136]. Biopolymers add different binding chemistry to a renewable, multifunctional chain. Cellulose hydroxyl groups bind Zn^{2+} more strongly than water (-2.94 vs -1.07 eV) and lowered the desolvation activation energy from 44.9 to 29.9 kJ mol^{-1} relative to the liquid electrolyte [137]. In PAM/carboxymethyl chitosan, carboxylate groups bound Zn^{2+} more strongly than the PAM amide (-0.19 vs -0.11 eV), hydrogen bonding converted free water into bound water, and $t_{(Zn^{2+})}$ rose from 0.47 for PAM to 0.62, then to 0.74 once tert-butylamine suppressed amino protonation [78]. The effect therefore depends on group type, density, and ionization state rather than on biological origin, and amino-rich CS can protonate and repel Zn^{2+}. Binding energies from different studies are not directly comparable, and no study has yet compared biopolymer and synthetic groups at equal group density. The continuous synthetic framework, meanwhile, holds those channels open over long-term cycling and prevents the structural collapse that degrades pure BPG electrolytes. Because the two effects act on different parts of the problem, one on the

Just Accepted

solvation environment, the other on channel continuity, conductivity, and cation selectivity can rise together rather than trade against each other [138]. Tannic-acid-sodium-alginate HB-SG electrolytes show the coordination chemistry involved, with Zn^{2+} bound simultaneously by alginate carboxyl and tannic-acid phenolic hydroxyl groups to form metal-ligand crosslinks [101, 139]. The conductivity and transference-number values that result are shown in Fig. 5(f). To improve the rate capability and cycle life of Zn-metal batteries, Wu et al. developed a zinc-coordinated chitosan electrolyte in which ionic crosslinking between Zn^{2+} and chitosan's amino and hydroxyl groups yields high Zn^{2+} conductivity (Fig. 5 (g)), uniform hexagonal zinc deposition, and 99.7% coulombic efficiency over 1000 cycles [47].

4.2.4 Dendrite Suppression and Cathode Dissolution Inhibition

Interface stabilization in HB-SG electrolytes operates through complementary chemical and physical routes. Chemically, biopolymer segments anchor onto the zinc surface through chelation and electrostatic interaction, creating a dense array of zincophilic sites that homogenize the interfacial electric field and Zn^{2+} flux, thereby guiding planar, epitaxial nucleation instead of tip-driven dendritic growth [140]. Fig. 5(h) shows that the interwoven network functions as a mechanical barrier that obstructs the vertical propagation of any dendrites that form. The Zn stripping/plating reactions cycled with HB-SG electrolytes are more likely to occur homogeneously across the electrode surface rather than at a concentrated point, thereby suppressing dendrite formation and leading to better cyclic stability [101].

4.2.5 Wide-Temperature Adaptability

The two components also cover opposite ends of the temperature range. Below zero, the biopolymer phase hydrogen-bonds strongly with water and converts free water into bound water that cannot organize into an ice lattice, which depresses the freezing point and keeps both ionic conductivity and flexibility intact in the cold. At elevated temperature, the covalently crosslinked synthetic network is expected to resist shrinkage and solvent loss, holding the gel dimensionally and electrochemically stable [141]. Neither component achieves this range alone, and the operating windows that follow from the combination are reported in Section 6.3. In an other case, at -30 ºC the CSAM gel in 2 m $Zn(ClO_4)_2$ retained 7.8 mS cm^{-1} and no ice band appeared in Raman spectra, whereas the polymer-free $Zn(ClO_4)_2$ solution formed salty ice and cells with it were open-circuit from the first cycle, while Zn||Zn with polymer gel ran for more than 1200 h at 0.5 mA cm^{-2} [66].

4.2.6 Mechanistic Basis of Hybrid Superiority

Just Accepted

The mechanisms above are most convincing where a hybrid gel is compared with its single-network parent under identical conditions, and the result is supported by calculation or spectroscopy. In each case, the hybrid outperformed its synthetic parent, and the gain coincided with changes that can be explained at the molecular or network level. Biopolymer-only controls are rarely reported. At the molecular level, the hybrid supplies Zn^{2+} ligands of different affinities. In the CS/PAM electrolyte of Yao et al., DFT binding energies of PAM (-1.24 eV) and glycerol (-1.09 eV) exceed that of water (-0.64 eV), and MD places PAM in the Zn^{2+} first shell, while chitosan -OH/-NH_2 and PAM -$CONH_2$ act as hydrogen bond donors that displace water around BF_4^-. The charge transfer activation energy falls from 43.53 to 27.02 kJ $mol^{-1,}$ and $t_{(Zn^{2+})}$ reaches 0.82 [135]. In PNMA/SA, coordination of Zn^{2+} by alginate carboxylate is proposed to reduce the water in the shell, and $t_{(Zn^{2+})}$ rises from 0.49 for PAM to 0.55 [123].

The two components also modify each other. In PAM/CMCS, MD shows the carboxymethyl chitosan chain collapsing through -NH_3^+-COO^- attraction, which buries carboxylate sites. When tert-butylamine suppresses amino protonation, the chain stays extended, SAXS gives a smaller and narrower network radius of gyration (35.6 nm against 45.4 nm for PAM), and $t_{(Zn^{2+})}$ rises from 0.47 to 0.74 [78]. Biopolymer groups therefore contribute only when the network and local chemistry keep them accessible, so the benefit belongs to the hybrid rather than to either parent. The response can also be non-monotonic. In PNMA/SA, bound water and conductivity peak together at an alginate/monomer ratio of 0.3 and fall at 0.35 as alginate agglomerates, consistent with a balance between channel formation and network connectivity[123].

At the electrode, the same chemistry changes nucleation. Zeng et al. report stable 3D diffusion within 5 s and strong (002) texture[123]. In PAM/CMCS, DFT adsorption energies of CMCS on $Zn_{(002)}$ (-2.22 eV parallel, -1.39 eV vertical) exceed those of water, and the corrosion current falls from 1.21 to 0.41 mA cm^{-2} [78]. These results link the solvation, network, and interfacial steps into one chain. Causal proof remains limited because DFT uses small models, binding energies cannot be compared across studies, and most controls are partial.

5. Advanced Fabrication Strategies

The diversified structural classifications and synergistic mechanisms of HB-SG electrolytes discussed in Section 4 are closely correlated with their fabrication methodologies.

Just Accepted

The rational selection of preparation routes directly determines network topology, crosslinking mode, component compatibility, and final comprehensive performance. This section elaborates four mainstream preparation strategies for HB-SG electrolytes, combining synthetic principles, process characteristics, representative research cases, and corresponding performance data.

5.1 Polymerization Hybridization

Polymerization hybridization is a dominant chemical route for constructing covalently crosslinked HB-SG networks. The general workflow starts by preparing a homogeneous precursor solution of synthetic monomers, initiators, chemical crosslinkers, natural biopolymers, and electrolyte salts. Polymerization is then triggered by heat, ultraviolet irradiation, or other external stimuli, enabling in-situ formation of a synthetic polymer network that interpenetrates the pre-existing biopolymer framework. This one-pot synthesis eliminates interfacial defects between the two polymer phases and ensures uniform distribution of liquid electrolyte throughout the nanoporous network. Fu et al. adopted this strategy to synthesize PSX HB-SG electrolyte. They first used ring-opening polymerization to graft carboxyl groups onto PVA backbones to obtain modified PS precursors, then introduced xanthan gum (XG) and employed glutaraldehyde as a crosslinker to realize covalent crosslinking between PS and XG. After soaking in 2 M $ZnSO_4$ for 48 h, the gel achieved an ionic conductivity of 18.86 mS cm^{-1} and a Zn^{2+} transference number of 0.8 [142]. Sun et al. further introduced ZrO_2 ceramic nanoparticles into the copolymerization system of acrylamide and 2-acrylamido-2-methylpropanesulfonic acid. The interaction between ZrO_2 and sulfonic acid groups built multi-channel ion-transport pathways, and the resulting HB-SG reached an ionic conductivity of 38.3 mS cm^{-1} [143]. Ahmed et al. combined a PAM/hemp-derived cellulose-nanofiber quasi-solid electrolyte with a cobalt-manganese oxide carbon-nanofiber cathode. Raising the nanofiber content to 1.0 wt% gave the highest electrolyte uptake and conductivity, the lowest plating/stripping overpotential, and the best dendrite suppression. Nanofibers were dispersed in water, and acrylamide was added together with N, N'-methylenebisacrylamide as a crosslinker, and polymerization was carried out. Because the monomer polymerises around and through the suspended fibrils rather than being blended into an already-formed gel, the PAM chains and cellulose nanofibers interpenetrate at the molecular level [89]. This method is particularly suitable for preparing integrated electrode-electrolyte assemblies with low interfacial resistance.

5.2 Dual-Network Sequential Gelation

Just Accepted

Dual-network sequential gelation is a targeted technique for constructing interpenetrating dual-framework HB-SG electrolytes through two sequential steps: first, a rigid synthetic polymer network is formed by polymerization or physical crosslinking as a pre-gel skeleton; then the pre-gel is immersed in a biopolymer precursor solution, allowing biopolymer chains to permeate the network voids and undergo secondary gelation, producing two mutually intertwined networks with distinct functional roles. Zeng et al. combined photopolymerization and ionic crosslinking to prepare PNMA/SA dual-network gels. UV-initiated radical polymerization first formed the rigid PNMA network; the pre-gel was then immersed in $Zn(ClO_4)_2$ solution containing SA, where Zn^{2+} triggered ionic crosslinking of SA to form the biopolymer network. The final gel combined a tensile strength of 838 kPa with an ionic conductivity of 33.1 mS cm^{-1} [123]. Chen et al. prepared agar/HPAAm dual-network PGE via sequential gelation; the composite withstood 30 stretching cycles at 500% strain and recovered nearly 100% of its original length [144]. Li et al. used the same strategy for lignin-cellulose/PAM dual-network gels, which reached a tensile strain of 1100%, with the assembled Zn//MgVO battery retaining 91.9% of its capacity after 4000 cycles at 5 A g^{-1} [105]. This method allows each network to be regulated independently, facilitating customized functional design.

5.3 Supramolecular Modification Hybridization

Unlike conventional covalent and ionic crosslinking, supramolecular modification builds hybrid networks from reversible interactions, such as hydrogen bonding, metal-ion coordination, and host-guest recognition. Synthetic polymers and biopolymers are pre-modified with specific recognition groups, and directional supramolecular assembly during gelation endows the gels with self-healing and stimulus-responsive behavior. Y Lin. et al. doping a trace of Fe^{3+} ions to afford Fe^{3+}-carboxylate supramolecular interaction, the practicality of an archetypal cellulose nanofiber-reinforced PGE is significantly improved in a couple of aspects, including three-fold and eight-fold increases in tensile strength and toughness without loss of ion-conducting ability (up to 32 mS cm^{-1}) and being room-temperature self-healable and strongly adhesive to various battery components [145]. Also reinforced the mechanical strength, giving autonomous self-healing at room temperature; after one cutting-healing cycle, the device recovered 96% of its original performance. Cao et al. used Li^+ and Ag^+ as coordination crosslinkers to construct chitosan supramolecular HB-SGs that remained structurally stable at 100 °C with excellent mouldability [146]. Such

Just Accepted

supramolecular HB-SG electrolytes are well suited to wearable and flexible zinc-ion energy devices.

5.4 Green Fabrication Approaches

For industrial translation, several eco-friendly, large-scale technologies have been developed, featuring low energy consumption, non-toxic raw materials, and continuous production, large-area solution casting, continuous UV curing, electrospinning, and freeze-casting.

As the most mature industrial route, solution casting extends laboratory coating to batch production. The mixed precursor solution is uniformly coated onto flexible substrates and dried into continuous gel films. Kasprzak et al. similarly used casting to prepare chitosan-based HB-SG electrolytes doped with ionic liquid or starch derivatives, illustrating compatibility with green processing principles, although these routes have so far been demonstrated only at laboratory scale rather than in continuous industrial production [147]. J. Wang et al. used solution casting derived from physical blending to prepare a sodium alginate/guar gum/EG HB-SG electrolyte. The system achieved a room-temperature ionic conductivity of 25.37 mS cm^{-1}, and a stable electrochemical response across varied temperatures and current densities [148]. Caldeira et al. prepared a biodegradable XG/PVA HB-SG electrolyte via a facile solution-casting technique by blending aqueous polymer solutions into uniform membranes. The best results were ionic conductivities of 1.97×10^{-4} and 7.41×10^{-4} S/cm at room temperature [149]. Wu et al. prepared a densified chitosan-Zn electrolyte by casting a chitosan solution (4 wt% chitosan in 4 wt% acetic acid) onto a PET support, immersing it in a Zn^{2+} saturated NaOH solution to coagulate the chitosan and load Zn^{2+} into the network, rinsing to neutral pH, and finally mechanically compressing the membrane at ~5 MPa to remove excess water and densify the structure. The resulting electrolyte was shown to be non-flammable, only shrinking and softening when exposed to flame, and its biodegradability was directly verified by soil burial, the membrane began visibly degrading (moldy, then decomposing) after 2 months and was fully degraded after 5 months, with an estimated manufacturing cost of ~\$4.2 m^{-2} (\$46.5 kg^{-1}), comparable to commercial separators [47]. This indicates that solution casting is a promising, scalable-in-principle approach for fabricating eco-friendly polymer electrolytes, though pilot- or production-scale validation for this specific system has not yet been reported.

Just Accepted

Roll-to-roll technology uses high-intensity UV light to trigger rapid gelation of precursor coatings, offering high efficiency and low pollution. Quan et al. modified wheat-straw cellulose with sorbitol and fabricated Sor-Cel HB-SG electrolyte by UV curing; the material reached an ionic conductivity of 35.4 mS cm^{-1} and remained stable in mechanical and electrochemical performance under twisting and bending at -40 °C [150]. Another technique is Electrospinning, which draws polymer solutions into nanofibrous membranes under a high-voltage electric field, giving a large specific surface area and uniform pore structure. Zhu et al. fabricated soy-protein-isolate (SPI)/PVA fibrous hybrid membranes by electrospinning through a pollution-free process; the activated gel electrolyte showed low interfacial resistance and good electrochemical activity [151].

Freeze-casting controls directional ice-crystal growth to build hierarchical pore structures inside the gel. Zhao et al. fabricated a BC/PVA HB-SG electrolyte through a freeze-thawing synthesis method, allowing bacterial cellulose microfibers to be uniformly integrated into the PVA network. Hydrogen-bond interactions between BC and PVA generated a robust dual-network structure, simultaneously enhancing mechanical strength and facilitating efficient ion transport [152]. Lu et al. prepared a chitosan/polyaspartic-acid (CPZ-H) electrolyte via a simple aqueous freeze-gelation route, where chitosan and polyaspartic acid were dissolved in an NaOH/urea alkaline solvent, combined with $ZnSO_4$, subjected to a freeze-thaw cycle, and gelled by heating at 60 °C, before soaking to neutral pH. The electrolyte is directly recyclable. Aged CPZ-H can be dried, ground to a powder, redissolved with a few drops of water, remolded, and reheated to yield a recovered electrolyte (rCPZ-H) that retained high electrochemical utility, supporting over 750 h of stable Zn/rCPZ-H symmetric cycling and 86.7% capacity retention after 2400 cycles in a full Zn||rCPZ-H||MnO_2 cell. Its biodegradability was verified through two independent, real-world case tests: one was incubation in a Bacillus culture, in which the electrolyte was progressively decomposed and had almost disappeared after 90 days, and burial in natural soil tracked photographically over time. The electrolyte was further demonstrated in practical mechanical roles, molded into a traction rope and a conveyor belt to power a small elevator and a model Ferris wheel, respectively, remaining structurally intact through repeated operation[153].

In summary, each preparation strategy suits distinct scenarios, in-situ polymerization and supramolecular modification target high-performance smart gels; physical blending and sequential gelation balance performance against fabrication difficulty; and green, potentially scalable technologies point toward future industrialization of HB-SG electrolyte-based zinc-

Just Accepted

ion energy storage devices. However, with the partial exception of solution casting, most examples above have been demonstrated only at laboratory scale, and genuine industrial scalability, cost, and environmental benefit remain to be validated at pilot or production scale.

6. Performance of HB-SG electrolytes

This section characterizes the multi-dimensional functional performance of HB-SG electrolytes for ZIBs. Building on the structural advantages and synergistic mechanisms of Section 4 and the fabrication routes of Section 5, we discuss ion transport, mechanical performance, temperature adaptability, smart functionality, and electrochemical stability of these hybrid systems.

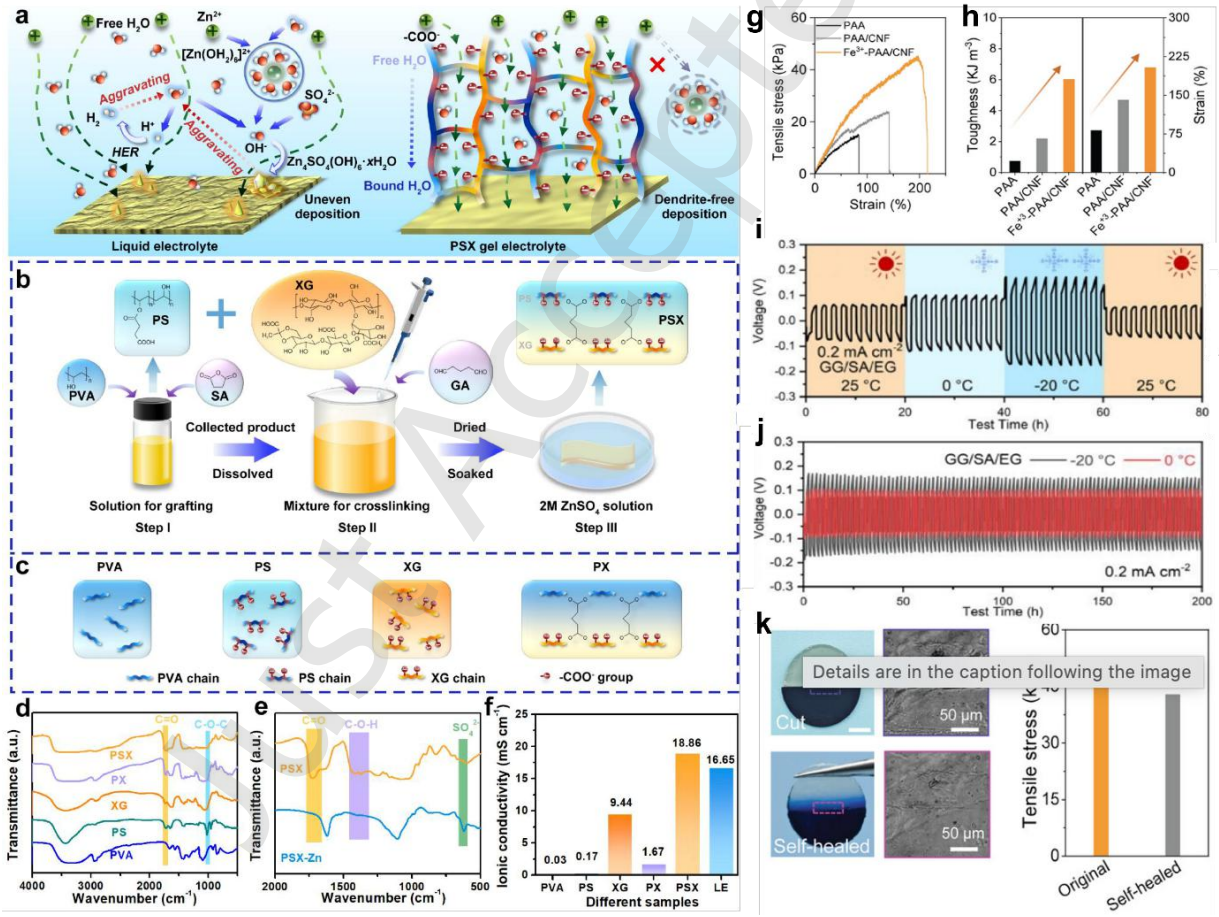


Figure 6. Structural design and performance of HB-SG electrolytes for dendrite-free Zn deposition, mechanical reinforcement, and low-temperature operation. (a) Schematic comparing Zn deposition in liquid electrolyte versus the PSX gel electrolyte. (b) Fabrication route in which PVA/SA is grafted with carboxyl groups via ring-opening of succinic anhydride (PS), then crosslinked with xanthan gum (XG) via glutaraldehyde (GA) and soaked in $ZnSO_4$ to form the PSX gel. (c) Schematic of PVA, PS, XG, and PX chain

Just Accepted

structures. (d, e) FTIR spectra of PVA, PS, XG, PX, and PSX/PSX-Zn showing characteristic bonds. (f) Ionic conductivity of PVA, PS, XG, PX, PSX, and the liquid electrolyte. Reproduced with permission [142]. (g) Tensile stress-strain curves of PAA, PAA/CNF, and Fe^{3+}-PAA/CNF gels. (h) Toughness and strain comparison across the same three gels. Reproduced with permission [145]. (i) Voltage profile under cyclic 25 °C/0 °C/-20 °C temperature switching at 0.2 mA cm^{-2}. (j) Voltage profiles at -20 °C and 0 °C over extended cycling. Reproduced with permission [148]. (k) Photographs and SEM images of the gel before and after cutting/self-healing, with corresponding tensile strength retention. Reproduced with permission [145].

6.1 Ionic Conductivity and Ion-Migration Regulation

Ionic conductivity and the Zn^{2+} transference number are the core electrochemical indicators of PGEs, directly determining the reaction kinetics and rate capability of ZIBs[154]. Ionic conductivity is obtained from,

$$\sigma = L / (R \cdot A) \quad (1)$$

where σ is the ionic conductivity, L the thickness of the gel electrolyte, R the bulk resistance, and A the effective test area. In an aqueous gel, both Zn^{2+} and the accompanying anions move, and excessive anion transport sets up internal fields that impede cation motion, so a high Zn^{2+} transference number matters as much as raw conductivity. HB-SG electrolytes improve on single-component systems on both counts, for the reasons given in Section 4.2.3, the interpenetrating synthetic-biopolymer framework provides continuous diffusion channels, both components act on the shell, and the biopolymer contributes complementary groups to the Zn^{2+} solvation shell and lowers the desolvation barrier [155, 156]. Benefiting from their complementary network structure, HB-SG electrolytes optimize both ion-transport channels and ion-solvation environments relative to single-component systems, the interpenetrating synthetic-biopolymer frameworks build hierarchical interconnected pores that provide continuous diffusion pathways.

The PSX system reported by Fu et al. shows clearly why the functional groups and the network have to work together [142]. The carboxylate groups anchor Zn^{2+} electrostatically and weaken its coordination with water, while the crosslinked framework supplies the continuous three-dimensional channels the ions travel through (Fig. 6(a)). Carboxyl groups were first grafted onto PVA through ring-opening of succinic anhydride to give PS, which was then crosslinked with xanthan gum using glutaraldehyde and soaked in 2 M $ZnSO_4$ (Fig.

Just Accepted

6(b)), with control gels carrying only one of the two features prepared alongside it (Fig. 6(c)). FTIR confirms both steps; the C=O band is strongest in PSX (Fig. 6(d)), and the C-O-H bending signal weakens after soaking as the carboxyl groups deprotonate and exchange with Zn^{2+} to form carboxylate (Fig. 6(e)). The conductivity data in Fig. 6(f) separate the two contributions: grafting alone (PS, 0.17 mS cm^{-1}) and crosslinking alone (PX, 1.67 mS cm^{-1}) both sit close to pristine PVA (0.03 mS cm^{-1}), whereas combining them yields 18.86 mS cm^{-1}, above the liquid electrolyte itself (16.65 mS cm^{-1}), with the Zn^{2+} transference number rising to 0.8 from 0.34.

Xia et al. combined PAM with pseudo-polyrotaxane structures; the single-ion transport mechanism gave 22.4 mS cm^{-1} with a Zn^{2+} transference number of 0.923 [157]. Zhang et al. developed P(AM-co-SBMA) gels whose dual-functional groups regulate cation and anion migration simultaneously, reaching 32.9 mS cm^{-1} and a transference number of 0.84 [158]. Another densified chitosan-Zn gel reaches 71.8 mS cm^{-1} and sustains rate capability up to 20 C [47]. Sun et al. prepared PVA-gelatin water-in-salt HB-SGs reaching 110.2 mS cm^{-1}, close to three times the value of 10 M $ZnCl_2$ solution (34.0 mS cm^{-1}) [127].

6.2 Mechanical Flexibility, Stretchability, and Anti-fatigue Behavior

The gel serves as electrolyte and separator at once; it has to tolerate repeated stretching, compression, and the volume changes of the electrodes. Crosslinking mode governs the outcome; physical crosslinks give flexibility with low rigidity, covalent crosslinks give strength with limited ductility, and hybrid networks combine the two, the complementation mechanism set out in Section 4.2.2. A useful demonstration of how far this complementation can be pushed comes from a cellulose-nanofiber-reinforced polyacrylic acid gel in which trace Fe^{3+} was introduced to form supramolecular Fe^{3+}-carboxylate crosslinks. The stress-strain curves in Fig. 6(g) separate the two contributions, adding cellulose nanofibers to bare PAA raises both the stress the network sustains and the strain it survives, and the subsequent Fe^{3+} coordination raises them again, giving roughly a threefold gain in tensile strength and an eightfold gain in toughness relative to unmodified PAA, with the same ordering reproduced in the toughness and fracture-strain bars (Fig. 6(h)). The mechanism is coordination rather than simple filler reinforcement. Fe^{3+} binds the carboxylate groups and promotes additional hydrogen bonding between polymer chains, so the network is tightened without blocking the conduction pathways. This is the point that matters for electrolyte use; ionic conductivity was retained at 32 mS cm^{-1}, so strength and transport were

Just Accepted

improved together rather than traded against each other. Also, the batteries operated under severe conditions of 180° folding and exposure to liquid nitrogen [145]. Wang et al. reported agar/HPAAm dual-network gels stretched to 500% strain over 30 consecutive cycles with almost complete recovery of the original length, indicating strong fatigue resistance [159]. Ma et al. obtained PANa-cellulose HB-SG electrolyte with 800% stretchability in bulk form and 500% in fiber-shaped devices [160]. Cao et al. tuned zinc-salt anions in gelatin-based HB-SGs through the Hofmeister effect; the $ZnSO_4$-soaked gel reached a breaking stress of 1.5 MPa, and the assembled cell ran for 9300 cycles [161]. Sequentially gelled PNMA/SA dual networks combined 838 kPa tensile strength with 33.1 mS cm^{-1}, showing that strength and conduction can be raised together [123]. Blended and supramolecular HB-SG electrolytes perform adequately by the same measures, with chain entanglement reinforcing the framework and dynamic bonds improving adaptability to deformation, which is what flexible and wearable cells require.

6.3 Wide Temperature Performance

Single-component gels operate over a narrow temperature range, SPG electrolytes dry out and shrink when hot and lose chain mobility when cold, while BPG electrolytes resist freezing but lack high-temperature stability. HB-SG electrolytes span both ends, for the reasons given in Section 4.2.5, and the reported windows are correspondingly wide. Zhang et al. prepared P(AM-co-DMAEMA)/gelatin organohydrogels that retained adhesion, resistance to drying, and deformability at -40 °C through prolonged twisting and stretching [162]. Wang et al. approached cold temperature operation with a guar gum/sodium alginate PGE modified with ethylene glycol (GG/SA/EG), and tested it in a way that separates two questions often run together: whether a gel still works when cold, and whether it survives having been cooled. Symmetric Zn cells were cycled at 0.2 mA cm^{-2} through a stepped sequence of 25 °C, 0 °C, -20 °C, and back to 25 °C (Fig. 6(i)). Polarization remained below roughly 200 mV at 25 and 0 °C and rose only to about 320 mV at -20 °C. More meaningfully, it returned to its starting value once the cell was rewarmed, indicating that freezing had not permanently damaged the network. Sustained operation followed at both low temperatures, with stable plating and stripping for over 200 h at 0 °C and -20 °C (Fig. 6(j)). The EG hydrogen-bonds with water and disrupts ice nucleation, while the guar gum and alginate chains bind free water, which is the free-versus-bound-water mechanism set out in Section 4.2.5 [148].

6.4 Self-healing and Anti-deformation Capability

Just Accepted

Self-healing matters for flexible and wearable cells because damage in service is difficult to avoid. When the gel is cut or torn, dynamic non-covalent bonds reconstruct the network without external stimulus, restoring both mechanical and electrochemical function. Most blended and supramolecular HB-SG electrolytes rely on reversible interactions between the synthetic and biopolymer chains to heal at room temperature. The Fe^{3+} carboxylate bonds that stiffen the PAA/CNF network (Section 6.2) are reversible, so the same chemistry that supplies strength also lets the gel repair itself. Fig. 6(k) shows a disc cut through with a scalpel rejoining once the two halves are held in contact, the healed piece supports its own weight when lifted with tweezers, while optical microscopy of a scratched surface shows the groove closing over time with no applied heat, light, or solvent. Recovery is close to complete, with tensile properties returning to 95% of the original value within 24 h. Dye tracing confirms the join is more than surface adhesion. Coomassie brilliant blue diffused from a stained block into an unstained one over the same period, indicating that polymer chains migrate across the interface and re-form coordination bonds. Healing without external stimulus is the practically relevant case, since a cell damaged in service cannot easily be heated or irradiated to trigger repair [145]. Hsu et al. built mussel-inspired GelMA/CNC/TA PGE in which hydrogen bonding between GelMA and tannic acid forms a double network, and cellulose nanocrystals supply reinforcement. After a single cutting and healing cycle at room temperature, the device recovered 96% of its original electrochemical performance [163]. Dual-network HB-SG electrolyte resists deformation by a different route, dispersing local stress so that large strain does not cause overall failure. Wu et al. prepared carrageenan/PAM gels in one pot, where heating at 95 °C with KCl induction drives carrageenan into a coiled structure intertwined with the PAM network, and the composite survived prolonged extrusion and bending without structural damage [164]. HB-SG electrolytes modified with cyclodextrin and related macrocyclic hosts add host-guest recognition as a further route to reversible reconstruction after fracture, which suits repeatedly deformed devices.

6.5 Recyclability and End-of-Life Recovery Strategies

HB-SG and BPG electrolytes can be recovered or retired through two end-of-life pathways that are largely unavailable to single-component SPGs, mechanical/material recycling and microbial biodegradation. This distinction is rooted in network chemistry rather than incidental processing choices. Gu et al. make this explicit for covalently crosslinked polymer electrolytes generally: “the employment of electrolytes comprising a covalent bond

Just Accepted

cross-linking matrix is considered as an effective strategy to improve the mechanical properties, thermal stability and inhibit dendrite growth. Cross-linked network cannot be processed after curing, nor can it be restored to use after battery failure [165]". Reprocessability was only restored by deliberately replacing permanent crosslinks with a dynamic, exchangeable imine-bond network (achieved here with a soy-protein isolate matrix, reshapeable and recyclable using only water at room temperature), demonstrating that recyclability in a polymer electrolyte is not an inherent property of the network but something that must be specifically engineered into it. A parallel asymmetry holds for biodegradation. In PAM-type synthetic hydrogels, soil microorganisms can use the amide side-groups as a nitrogen source, but the remaining carbon-carbon backbone is recalcitrant: its long, hydrophobic chain geometry leaves few reactive terminal groups for microbial enzymes to act on, so degradation proceeds slowly and typically requires deliberate inoculation with specific bacteria or fungi, reaching only 0.12-7.3% mass loss over 2-9 months under most reported conditions (rising to 31-78% only with targeted microbial strains) [166]. By contrast, biopolymer backbones built on glycosidic linkages (cellulose, starch, alginate, chitosan) present many internally accessible cleavage sites that native soil/gut microorganisms degrade without inoculation, which is consistent with the 90 days. Bacillus-driven degradation of CPZ-H and the 2-5 months soil-burial degradation of the chitosan-Zn electrolyte reported above [47, 153]. Together, this explains why BPG and biopolymer-rich HB-SG electrolytes can rely on ordinary soil disposal, whereas PAM-based HB-SGs would leave a non-degradable fraction, and SPGs built on permanent covalent networks and recalcitrant carbon backbones default to incineration or landfill unless redesigned with dynamic bonds.

7. Applications and Multifunctional Performance for Next-generation ZIBs

HB-SG electrolytes integrate the merits of natural biopolymers and synthetic polymers, offering mechanical flexibility, tunable ion transport, extreme-temperature tolerance, strong interfacial regulation, and multifunctional adaptability. Building on the structural design, functional characteristics, and synergistic mechanisms of the previous sections, this section examines their advanced application scenarios in ZIBs, suppression of parasitic reactions and cathode dissolution, expansion of the electrochemical window, wearable and flexible devices under extreme-temperature and harsh-condition operation, and compatibility with the four mainstream cathode families.

Just Accepted

7.1 Suppression of Parasitic Reactions and Cathode Dissolution

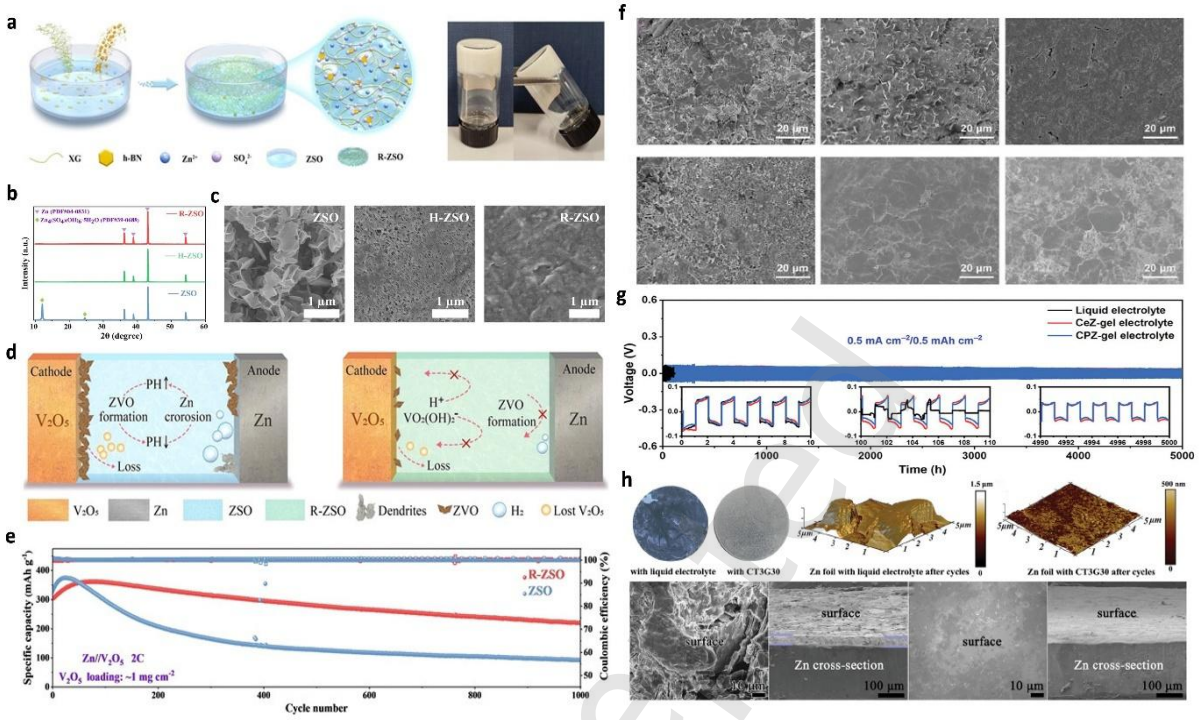


Figure 7. XG/h-BN-based ZSO gel electrolyte for suppressing parasitic reactions and V_2O_5 cathode dissolution in Zn batteries. (a) Schematic of the R-ZSO gel electrolyte preparation from XG, h-BN, Zn^{2+}, and SO_4^{2-}, and photographs of the resulting flexible gel. Reproduced with permission. (b) XRD patterns of ZSO, H-ZSO, and R-ZSO. Reproduced with permission. (c) SEM images of Zn foil surfaces after cycling with ZSO, H-ZSO, and R-ZSO surface morphology. Reproduced with permission. (d) Schematic comparison of Zn/V_2O_5 cell degradation mechanisms with ZSO versus R-ZSO. Reproduced with permission. (e) Cycling performance of $Zn//V_2O_5$ cells with ZSO and R-ZSO electrolytes. Reproduced with permission [167]. (f) SEM images of Zn foil surfaces after cycling with different CPZ gel electrolytes. Reproduced with permission. (g) Voltage profiles of liquid, CeZ-gel, and CPZ-gel electrolytes. Reproduced with permission [168]. (h) Photographs, AFM topography, and SEM cross-sectional images of Zn foil surfaces with liquid electrolyte versus CT3G30 gel electrolyte, before and after cycling. Reproduced with permission [169].

Aqueous ZIBs are plagued by parasitic reactions, HER, OER, zinc-anode corrosion and passivation, and cathode dissolution, originating from the high activity of free water and unstable electrode-electrolyte interfaces. The principal anode-side reactions in acidic, alkaline, and neutral media are:

Just Accepted

(1) $Zn + 2H^+ \rightarrow Zn^{2+} + H_2\uparrow$

(2) $Zn + 2OH^- \rightarrow ZnO_2^{2-} + H_2\uparrow$

(3) $Zn \rightarrow Zn^{2+} + 2e^-$

(4) $2H_2O + 2e^- \rightarrow H_2\uparrow + 2OH^-$

(5) $2H_2O \rightarrow O_2\uparrow + 4H^+ + 4e^-$

(6) $4Zn^{2+} + SO_4^{2-} + 6OH^- + xH_2O \rightarrow Zn_4SO_4(OH)_6 \cdot xH_2O$

HB-SG electrolytes use the abundant polar groups of biopolymers to form dense hydrogen bonds with free water, reducing water activity and inhibiting HER/OER, while the network acts as both a physical barrier and chemical regulator. Biopolymer segments adsorb on the zinc surface via chelation and electrostatic interaction to induce uniform deposition, and the synthetic framework blocks dendrite growth. Wang et al. developed a fast-conducting Zn^{2+} hydrogel electrolyte (R-ZSO), which aims to solve the problems of uneven zinc deposition and positive and negative pole crosstalk in Zn/V_2O_5 cells. The polymer matrix and h-BN nanosheets can firmly anchor SO_4^{2-} ions, thereby promoting the migration of Zn^{2+} and forming dense and uniform zinc deposition. In addition, R-ZSO inhibits the migration of positive electrode-derived materials and reduces the corrosion of zinc, hydrogen evolution reaction, and the generation of zinc vanadate by-products. Therefore, Zn//Zn symmetric batteries using R-ZSO can operate stably for over 1500 hours, which is about six times that of batteries using blank electrolytes. In $Zn//V_2O_5$ full cell, R-ZSO electrolyte remained stable after 1000 cycles at 2C rate, demonstrating its effectiveness in improving long-term interface stability (Fig. 7(a-e)) [167]. Park et al. built an agarose-based protective layer on the zinc anode that isolated the metal from the bulk electrolyte, mitigated corrosion and passivation, and realized dendrite-free deposition (Fig. 7(f)) [170]. On the cathode side, the compact 3D network confines dissolved metal ions from Mn and V-based cathodes (Fig. 7(d)). Zhang et al. compared the liquid electrolyte, CeZ gel electrolyte, and CPZ gel electrolyte to clarify their effects on the zinc anode and PNZ cathode. CPZ gel electrolyte achieves stable zinc deposition/stripping for more than 5000 hours at current densities of 0.5 mA cm^{-2} and 0.5 mAh cm^{-2} (Fig. 7(g)). SEM analysis showed that CPZ gel effectively inhibited the accumulation of ZSH sheet on the two electrodes, and its rich hydroxyl group reduced the pH fluctuation and inhibited the hydrogen evolution reaction (Fig. 7(f)), and the assembled Zn‖phenazine battery operated stably for over 100 cycles at 311 mAh g^{-1} [168]. Chen et al.

Just Accepted

compared the morphology of zinc foil after 500 cycles in liquid electrolyte and CT3G30 gel electrolyte. The zinc foil circulating in the liquid electrolyte turns black and has a highly rough surface, indicating severe interface degradation and uneven zinc deposition. In contrast, the zinc foil protected by CT3G30 maintains its original appearance and has a noticeably smoother surface, as confirmed by atomic force microscopy and scanning electron microscopy (SEM) analysis (Fig. 7(h)) [169].

Just Accepted

7.2 Wearable, Flexible, Extreme Temperature and Harsh Condition ZIBs

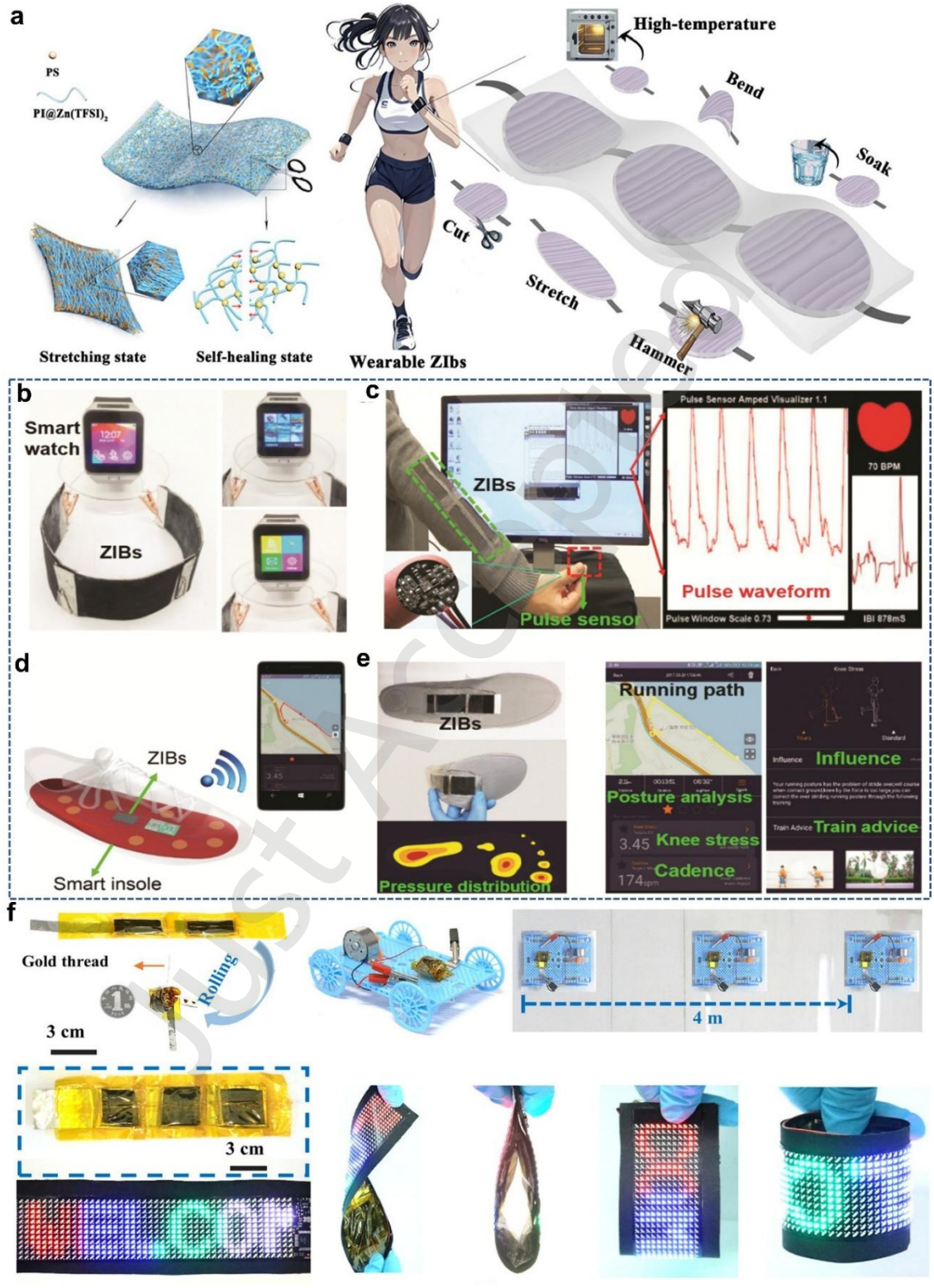


Figure 8. Wearable, flexible, and extreme condition tolerant ZIBs. (a) Schematic of a PI@Zn(TFSI)$_2$ hydrogel electrolyte in stretching and self-healing states, and a wearable ZIB

demonstrating tolerance to cutting, stretching, bending, high-temperature exposure, and soaking. Reproduced with permission [171]. Wearable demonstrations: (b) smart watch, (c) pulse sensor with waveform output, (d) Bluetooth-connected smart insole schematic, and (e) insole under bending with pressure mapping and tracked running data. Reproduced with permission [172]. (f) Photographs and demonstrations of a wearable battery integrated into a vehicle and powering an LED matrix display over a 4 m wireless range, with additional images showing the battery under bending, folding, and wearable-band configurations driving multicolor LED screen. Reproduced with permission [173].

Wearable electronics and flexible devices demand power sources that tolerate bending, stretching, sewing and repeated deformation. Combining the flexible biopolymer network with robust synthetic support, HB-SG electrolytes have become a core material for flexible ZIBs. The examples below vary in how rigorously deformation tolerance was tested: where the source study reports a specific number of bending/folding cycles and the corresponding capacity retention, this is stated explicitly; where a cell is reported only to operate, or to have been demonstrated, under a deformed state without a cycle count, this reflects a single or limited demonstration rather than validated cycling durability, and reliability claims below are limited accordingly. Chen et al. made a cotton-cellulose HB-SG electrolyte (CT3G30) using tetraethyl orthosilicate as crosslinker and glycerol as anti-freezing agent; the $Si(OH)_4$ generated on hydrolysis forms siloxane bonds with cellulose and glycerol, giving a gel that suppresses dendrites and side reactions from -40 °C to 60 °C. Deformation tolerance was tested under a defined protocol. After 60 cycles in the flat state at -40 °C, the quasi-solid Zn-MnO_2 cell was bent and cycled for a further 60 cycles, retaining 98% of the capacity measured in the unbent state at the same temperature [169]. Li et al. designed an elastic polymer salt electrolyte based on a polystyrene-block-polyisoprene (SIS) matrix containing 80 wt% $Zn(TFSI)_2$. Polyimide (PI) segments coordinate with the salt while polystyrene (PS) domains act as physical linkers, achieving high ionic conductivity (1.89×10^{-4} S cm^{-1}), a high Zn^{2+} migration number (0.83), and an elongation at break of 842%. The electrolyte also exhibits thermally activated self-healing behavior, allowing the all-solid-state zinc-ion battery to maintain a capacity of 106 mAh g^{-1} after 400 cycles and operate stably at temperatures up to 70 °C. Deformation tolerance was evaluated through a defined series of destructive tests rather than a single demonstration, under repeated bending (measured every 20 folds), the device retained 84.2% of its initial voltage after 120 bending cycles, under stretching, it retained 77.2% of its initial voltage after 5 stretching cycles; when cut in half, the open-

Just Accepted

circuit voltage retained 84.2% of its pre-cut value after 5 h of continued exposure and under continuous water immersion, it retained 95.8% of its initial voltage after 100 min (Fig. 8(a)) [171]. Wang et al. developed a sewable Zn-MnO_2 battery based on NFC/PAM PGE (60-180 μm pores), it retained 88.5% capacity after 120 sutures, withstood shear force above 43 N, and powered an LED when worn on a toy [131]. Wu et al. produced densified chitosan-Zn electrolytes (71.80 mS cm^{-1}, rate capability to 20 C, 400 cycles, fully soil-degradable) [47]. The carboxymethyl-chitosan/PAM (CSAM) gel of Huang et al. relies on ternary ClO_4^--water-polymer hydrogen bonds, giving 7.80 mS cm^{-1} and flexibility at -30 °C for Zn/PANI cells.[66] Li et al.'s gelatin/PAM hierarchical polymer electrolyte was demonstrated across three wearable applications with specific device configurations and outcomes. Three ZIBs (4 x 6 cm) connected in series powered a commercial Android smartwatch, which operated normally across all functions, including viewing pictures, accessing messages, and performing calculations (Fig. 8(b)). Four ZIBs (2 x 6 cm) connected in series and integrated into a T-shirt powered a pulse sensor, successfully detecting the pulse waveform under both flat and bent conditions (Fig. 8(c)). Two ZIBs (2.7 x 3.6 cm) placed beneath a commercial smart insole powered a Bluetooth-connected plantar measurement system, which operated without power failure or short-circuiting while the wearer walked, ran, or jumped; the system remained functional over a continuous outdoor run of 2.1 km and up to 80,000 steps of walking, transmitting gait, knee-stress, and cadence data to a mobile app throughout (Fig. 8(d), (e)) [172].

Multi-polymer systems optimize overall performance. Dual-crosslinked PAM/gelatin/SA PGE showed concomitantly reducing the freezing point and mitigating water loss, thereby giving the PGE improved adaptability to diverse operating conditions, balancing conductivity, flexibility, and stability [174]. Shao et al.'s carrageenan/wool-keratin (CWK) gel, with selective ion permeability, suppressed $Zn_4SO_4(OH)_6.H_2O$ by-product formation at the NVO cathode and kept the Zn-NaV_3O_8 (NVO) cell stable under a defined deformation protocol, at a fixed 1 cm bending radius, the cell retained 90% of its capacity after 100 bending cycles, compared with 96% retention under static (undeformed) cycling over 500 cycles [175].

Under harsh mechanical loads, extrusion, impact, twisting, cutting, and static pressure, dual-crosslinked, interpenetrating, and supramolecular HB-SG electrolytes provide toughness, anti-fatigue, and self-healing. Huang et al.'s SA/PAM gel was shown to withstand continuous treading and rolling without visible failure in the reported demonstration [176]. Luo et al.

Just Accepted

fabricated a multidirectionally deformable zinc-polyiodide battery (ZPPWIB) by constructing an oriented PEDOT:PSS conductive framework on a porous wood template. Hydrogen-bond-mediated self-assembly provided stable electron/ion pathways and retained electrical conductivity after 5000 bending cycles at a 180 ° angle and 6 months of water immersion. The assembled battery delivered a high areal capacity of 3.2 mAh cm^{-2} and an energy density of 3.8 mWh cm^{-2} and retained an areal capacity of 1.9 mAh cm^{-2} even under high current operation at 20 mA cm^{-2}. As shown in Fig. 8(c), two small ZPPWIBs connected in series could be rolled into a cylinder with a radius below 1 cm and stably power a toy car over a distance of 4 m, and three ZPPWIBs connected in series powered a flexible display during bending, twisting, and rolling [173]. These results highlight the potential of flexible ZIBs as robust power sources for wearable and deformable electronics.

7.3 Compatibility with Different Cathode Systems

The diverse networks, functional groups, and ion-regulation capabilities of HB-SGs enable good matching with the mainstream ZIB cathode families, inhibiting cathode dissolution, stabilizing interfaces, and optimizing ion transport.

Table 2. HB-SG electrolytes compatibility with different cathode systems and electrochemical performance in ZIBs.

Cathode	HB-SGs	Liquid electrolyte	σ (mS cm^{-1})	Tensile Strength (kPa)	Specific capacity	Cycles performance	Ref.
Zn//MnO_2	NFC/PAM	2 M $ZnSO_4$ + 0.2 M $MnSO_4$	22.8	158	260 mAh g^{-1} at 1 C	88.3% retention after 1000 cycles at 1C	[131]
Zn//MnO_2	GG/SA/EG	2 M $ZnSO_4$ + 0.1 M $MnSO_4$	25.37	n/a	354.9 mAh g^{-1} at 0.15 A g^{-1}	91.52% retention over 1000 cycles at 6 A g^{-1}	[148]
Zn//MnO_2	Gelatin/PAM	1 M $ZnSO_4$ + 0.1 M $MnSO_4$	17.6	7760	306 mAh g^{-1} at 1.6 mA g^{-1}	97% retention after 1000 cycles at 2772 mA g^{-1}	[172]
Zn//MnO_2	CMC/PAM	2 M $ZnSO_4$ + 0.1 M $MnSO_4$	13.03	33	245.39 mAh g^{-1} at 0.154 mA cm^{-2}	90.18% retention after 500 cycles at 0.308 mA cm^{-2}	[177]

Just Accepted

$Zn//MnO_2$	SA/PAM	2 M $ZnSO_4$ + 0.1 M $MnSO_4$	43.2	51.83	300.4 mAh g^{-1} at 0.11 A g^{-1}	82% retention after 500 cycles at 0.88 A g^{-1}	[178]
$Zn//MnO_2$	Carboxymethyl chitosan/PAM	2 M $ZnSO_4$ + 0.1 M $MnSO_4$ + 2 M LiCl	5.6	67	214.2 mAh g^{-1} at 0.5 A g^{-1}	75% retention after 500 cycle at 4 A g^{-1}	[179]
$Zn//MnO_2$	Gelatin/silk protein/PGA/Ag	2 M $ZnSO_4$ + 0.1 M $MnSO_4$	5.68	4500*	311.7 mA h g^{-1} at 0.2 C	94.6% retention after 100 cycles 61.6 mA g^{-1}	[180]
$Zn//MnO_2$	Xanthan gum/CNF/PAM	2 M $ZnSO_4$ + 0.1 M $MnSO_4$	28.8	84	237 mA h g^{-1} at 1 C	86.2% retention after 1000 cycles at 4 C	[181]
$Zn//MnO_2$	Chitosan/polyaspartic acid	2 M $ZnSO_4$ + H_2SO_4	5.51	53.2	523.6 mAh g^{-1} at 0.1 A g^{-1}	92.5% retention after 5000 cycles at 5 A g^{-1}	[153]
$Zn//Na_{0.65}Mn_2O_4.H_2O$	SA/PAM	1 M $ZnSO_4$ + 0.2 M $MnSO_4$	29.2	~500	305 mAh g^{-1} at 0.1 A g^{-1}	96% retention after 1000 cycles at 2 A g^{-1}.	[182]
Zn//PANI	Carboxymethyl chitosan/PAM	2 M $Zn(ClO_4)_2$	23.61**	~33.4	156 mAh g^{-1} at 0.1 A g^{-1}	2500 cycles at 5 A g^{-1}	[66]
Zn//PANI	Chitosan/PAM	$Zn(CF_3SO_3)_2$	11.6	80	219.3 mAh g^{-1} at 1 A g^{-1}	94.6 % retention after 2000 cycles at 3 A g^{-1}	[183]
$Zn//VO_2$	ChNF/PAM	1 M $Zn(CF_3SO_3)_2$	15.2	~115	263.9 mAh g^{-1} at 0.2 A g^{-1}	90.7% retention after 1000 cycles at 10 A g^{-1}	[184]
$Zn//V_2O_5$	Xanthan gum/PVA	2 M $ZnSO_4$	18.86	n/a	210 mAh g^{-1} at 0.1 A g^{-1}	46% retention after 3000 cycles at 0.5 A g^{-1}	[142]

**with water vapors, **at room temperature*

Manganese oxides (α-MnO_2, δ-MnO_2) offer low cost and abundant resources but suffer Mn dissolution and structural collapse [185]. Xu et al. used nanocellulose/CMC hybrids whose carboxyl groups bind free water and stabilize the cathode, giving stable cycling over 500 cycles at 8 C [48]. Lu et al.'s chitosan-polyaspartic-acid (CPZ-H) gel (5.51 mS cm^{-1}, 1298% fracture strain) let the Zn-MnO_2 cell retain 92.5% capacity after 5000 cycles

Just Accepted

at 5 A g^{-1} with no obvious Mn dissolution [153], and Zhang et al.'s urea-modified SA electrolyte optimized Zn^{2+} solvation for a stable screen-printed Zn-MnO_2 flexible cell [186].

Vanadium cathodes offer high capacity but suffer from ion dissolution and poor conductivity; biopolymer polar groups coordinate vanadium ions to restrain loss. Shao et al.'s carrageenan/wool-keratin (CWK) gel with Zn-NaV_3O_8 keeps a flexible cell working after bending, folding, squeezing, rolling, and compressing, retaining 99% capacity, compared with 96% retention under static cycling over the same 500 cycles [175]. Yang et al.'s bacterial-cellulose membranes fixed free water to suppress side reactions and dendrites in Zn-NVO cells [187]. Another HB-SGs showed practical and excellent climate adaptability. Wang et al. reported that a PGE formula utilizing ClO_4^- anions and hydrophilic -NH_2 on polyacrylamide chains is shown to bond with water molecules, while the zincophilic glucose preferentially regulates Zn^{2+} solvation. ZIBs operate in a wide temperature range and achieved high specific capacities of 488 and 254 mAh g^{-1}, and the pouch battery delivered 438.1 mAh g^{-1} and also completed 400 cycles at 200 mA g^{-1} [188]. Organic cathodes (PANI, quinones) are light, low-toxicity, and eco-friendly, and pair well with interfacial-compatible hybrids. Zhang et al.'s dual-crosslinked cellulose (DCZ-gel, 38.6 mS cm^{-1}, tensile strength 2.08 MPa) coordinated Zn^{2+} through cellulose carboxyl for uniform deposition, and the Zn-PANI cell delivered 160 mAh g^{-1} at 0.5 A g^{-1} and retained 85% capacity after 2000 cycles at 2 A g^{-1} [137]. Zn-I batteries offer high capacity but suffer from polyiodide shuttling, dendrites, and HER/OER. Huang et al. prepared a hybrid water reducer gel electrolyte (polyacrylamide (PAM)-polynaphthalene sulphonate (FDN)-carboxylated chitosan (CCS)/zinc sulfate (ZSO)). Zn-I_2 full cells employing this multifunctional gel electrolyte achieved outstanding cycling stability, retaining 118.5 $mAhg^{-1}$ after 9000 cycles at 5 Ag^{-1} [189].

In summary, HB-SG electrolytes break the performance limits of single-component materials. Their flexibility, extreme-temperature resistance, harsh-condition stability, and universal cathode compatibility drive the diversified development of ZIBs across wearable electronics, extreme-environment equipment, and transient/implantable devices, making them core candidates for next-generation high-performance, multifunctional aqueous zinc-ion batteries.

8. Conclusion and Future Perspectives

Just Accepted

HB-SG electrolytes offer a promising route to improve the safety, interfacial stability, and mechanical adaptability of aqueous zinc-ion batteries. By combining the abundant functional groups and renewable character of biopolymers with the controllable networks of synthetic polymers, these electrolytes can regulate water activity and Zn^{2+} transport, maintain electrode contact, and suppress dendritic deposition and parasitic reactions. Nevertheless, most reported systems have been evaluated in small laboratory cells under controlled conditions. Differences in electrolyte composition, gel thickness, cathode loading, Zn utilization, and testing protocols also complicate direct comparison. Further development should therefore shift from empirical formulation toward mechanism-guided design and practical cell validation, summarized schematically in Fig. 9.

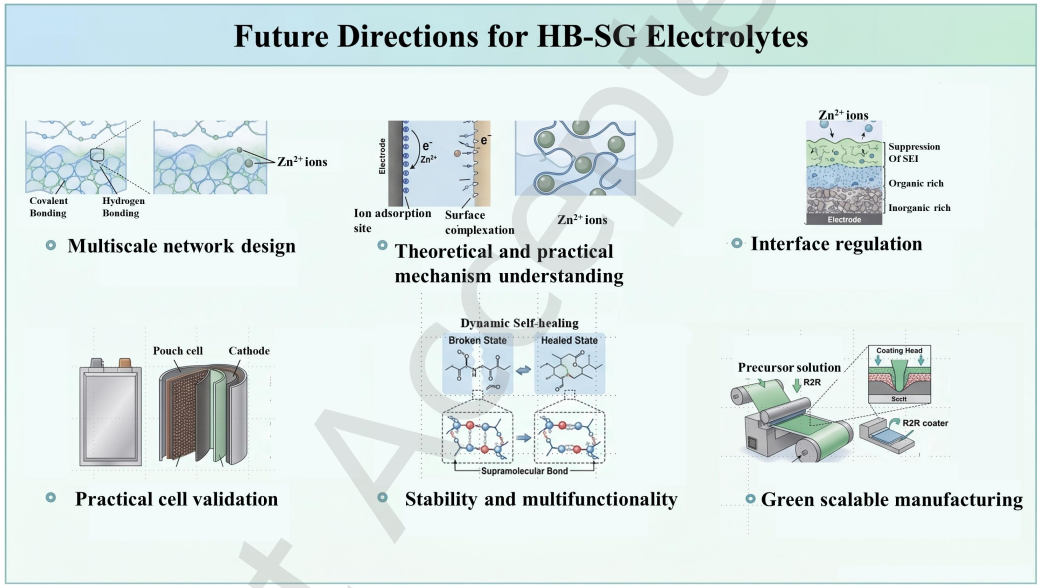


Figure 9. Schematic of HB-SG electrolytes for future direction. (Some parts were generated with the assistance of AI, subsequently reviewed and edited for scientific accuracy.)

Existing HB-SG electrolytes are commonly prepared by direct blending or conventional double-network construction, giving limited control over polymer distribution and crosslinking density. A corresponding strategy could require more precise control over the multiscale structure of HB-SG. Existing materials are commonly prepared by direct blending or conventional double-network construction, providing limited control over polymer distribution, crosslinking density, and phase compatibility. At the molecular level, the density and distribution of coordinating groups should be adjusted to regulate hydrogen bonding, Zn^{2+} coordination, and polymer-chain interactions. At larger scales, pore

Just Accepted

connectivity, water distribution, and interpenetrating or gradient networks can be designed to balance ionic transport, mechanical strength, water retention, and interfacial adhesion.

The other challenge is that the causal relationships among network chemistry, Zn^{2+} solvation, ion transport, and interfacial reactions remain insufficiently understood, and synergy is often proposed rather than directly demonstrated (Section 4.2). The relationships among network chemistry, Zn^{2+} solvation, ion transport, and interfacial reactions remain insufficiently understood. Unclear synergistic mechanisms could be addressed by density functional theory and molecular dynamics simulations, which can clarify interactions among Zn^{2+}, water, anions, and polymer functional groups, while finite-element analysis may reveal stress distribution and network damage under deformation and temperature variation. These predictions should be validated using in situ or operando spectroscopy and interfacial imaging. Combining theoretical calculations with experimental characterization would provide a more reliable basis for electrolyte design than mechanisms inferred solely from ex situ measurements.

Furthermore, bulk ionic conductivity alone cannot describe electrolyte performance, and many HB-SG electrolytes still trail liquid electrolytes at room temperature. As a path forward, ionic transport and electrode-electrolyte interfaces should be considered as coupled factors. Bulk ionic conductivity alone cannot adequately describe electrolyte performance; Zn^{2+} transference, desolvation kinetics, concentration polarization, water activity, and interfacial resistance are also important. Salt composition, functional-group density, ion-transport channels, and functional additives may be optimized to enhance Zn^{2+} mobility while limiting free-water activity. At the anode, the electrolyte should promote uniform Zn deposition and suppress corrosion, hydrogen evolution, and dendrite formation. At the cathode, it should maintain interfacial contact, reduce active-material dissolution, and inhibit the accumulation of insulating byproducts.

As discussed in Section 5.4, most green fabrication routes remain laboratory-scale, and batch consistency of biomass-derived components is not yet established. Scalable and environmentally responsible preparation remains essential for future research direction. Although agricultural and marine biomass may reduce raw-material costs, variations in purity, molecular weight, and functional-group content can affect batch consistency. Standardized extraction and purification procedures are therefore needed. Water-based processing, benign crosslinkers, one-pot gelation, continuous casting, and roll-to-roll manufacturing could

Just Accepted

simplify production and reduce energy consumption. Process development should also address gel thickness, electrolyte loading, curing time, mechanical defects, cost, and compatibility with existing battery-manufacturing lines. End-of-life should be designed alongside performance: dynamic crosslinks that allow recycling, and degradation rates measured under realistic conditions, should be reported for HB-SG electrolytes that contain non-degradable synthetic fractions such as PAM.

Dehydration, salt crystallization, and network ageing can degrade gel performance during storage rather than during operation. For this, long-term stability and multifunctionality require further evaluation. Dehydration, salt crystallization, network ageing, and freeze-thaw damage can alter the mechanical properties and ionic conductivity of gel electrolytes during storage. Shelf-life testing and effective water-retention and packaging strategies should therefore become part of routine assessment. Self-healing, temperature-responsive, electrochromic, and pressure-sensitive functions may broaden the applications of HB-SGs. However, their benefits must be evaluated against possible losses in electrochemical stability, mechanical integrity, and cycling performance.

Overall, the advancement of HB-SG electrolytes will depend on establishing quantitative relationships among network structure, ion transport, interfacial chemistry, mechanical behavior, and manufacturing conditions. Standardized testing, operando characterization, multiscale modeling, and validation in practical cell configurations will be critical for translating laboratory progress into safe, durable, and sustainable zinc-ion batteries.

9. Concluding Remarks

This review systematically surveys pure SPG, BPG, and HB-SG electrolytes for zinc-ion batteries, covering material systems, synergistic mechanisms, preparation technologies, functional properties, and practical applications. Natural biopolymers, such as cellulose, chitosan, sodium alginate, gelatin, and carrageenan, offer biodegradability, biocompatibility, and interfacial regulation that effectively suppress zinc dendrites and parasitic side reactions, but single-component biopolymer electrolytes are limited by insufficient mechanical strength, poor structural stability, and low ionic conductivity. Synthetic matrices such as PAM and PVA provide robust networks and good ion transport, yet suffer from non-degradability and weak electrode regulation. HB-SG electrolytes, built by a rational combination of the two, achieve complementary advantages and mutual defect offset. Across four structural families

Just Accepted

(dual-network, blended composite, supramolecular crosslinked, and organic-inorganic reinforced gels) and diverse preparation strategies, they deliver comprehensive gains in mechanical flexibility, fatigue resistance, wide-temperature adaptability, ion-migration efficiency, and electrochemical stability, together with good compatibility with manganese-, vanadium-, organic-, and iodine-based cathodes, and have been applied in wearable, extreme-temperature, and harsh-condition energy storage. Significant challenges remain; the microscopic synergistic mechanisms of multi-component networks are not fully clarified; room-temperature conductivity needs further improvement; long-term dehydration and storage instability persist; and large-scale industrial preparation is not yet mature. Addressing these through multi-scale structural design, combined theory and experiment, green industrial processing, intelligent multifunctional materials, and emerging applications will allow HB-SG electrolytes to become one of the most competitive core materials for next-generation safe, green, and multifunctional aqueous zinc-ion batteries.

Data availability

No primary research results, software or code have been included and no new data were generated or analyzed as part of this review.

Acknowledgements

This work was supported by the Natural Science Foundation of Anhui Province (No. 1908085QE225), the Open Project Program of State Key Laboratory of Molecular Engineering of Polymers (Fudan University) (No. K2024-12)

Declaration of competing interest

There are no conflicts to declare.

Author contribution statement

Adnan Ahmed: Writing original draft, data collection, Visualization, Muhammad Ali: Data curation and editing. Nishant Yadav: review & editing. Yinchun Fang: Formal analysis, Writing, review & editing. Xinhua Liu: Writing, review & editing, Supervision, Formal analysis.

Use of AI statement

AI-assisted tools were used for visualization and some parts of some figures, mostly redrawn and all based on actual data and drawn from the cited references.

References

[1] Aziz, A.;Ahammad, A. S.; Rahman, M. Preface to the Special Issue on Recent Advances in Electrochemical Energy Storage. *Chem. Rec.* **2024**, *24*, e202300358.

[2] Zhang, H.; Ma, Y. Topic "Electrochemical Energy Storage Materials"—An Overview. *Energies* **2025**, *18*, 1279.

[3] Armand, M.; Tarascon, J.-M. Building better batteries. *nature* **2008**, *451*, 652–657.

[4] Larcher, D.; Tarascon, J.-M. Towards greener and more sustainable batteries for electrical energy storage. *Nat. Chem.* **2015**, *7*, 19–29.

[5] Xu, K. Electrolytes and interphases in Li-ion batteries and beyond. *Chem. Rev.* **2014**, *114*, 11503–11618.

Just Accepted

[6] Shahzad, S.;Shah, A.;Kowsari, E.;Iftikhar, F. J.;Nawab, A.;Piro, B.;Akhter, M. S.;Rana, U. A.; Zou, Y. Ionic liquids as environmentally benign electrolytes for high‐performance supercapacitors. *Glob. Chall.* **2019**, *3*, 1800023.
[7] Ray, A.; Saruhan, B. Application of ionic liquids for batteries and supercapacitors. *Materials* **2021**, *14*, 2942.
[8] Zhou, D.;Shanmukaraj, D.;Tkacheva, A.;Armand, M.; Wang, G. Polymer electrolytes for lithium-based batteries: advances and prospects. *Chem* **2019**, *5*, 2326–2352.
[9] Sun, S.;Guan, Z. K.;Feng, Y. H.;Hu, L. J.;Zhang, X. Y.;Liu, M.; Wang, P. F. High‐Safety Design of Organic Electrolytes for Sodium‐Ion Batteries. *ChemSusChem* **2025**, *18*, e202501336.
[10] Ningappa, N. G.;Madikere Raghunatha Reddy, A. K.; Zaghib, K. Advanced polymer electrolytes in solid-state batteries. *Batteries* **2024**, *10*, 454.
[11] Agnihotri, T.;Ahmed, S. A.;Tamilarasan, E. B.;Hasan, R.;Su, W. N.; Hwang, B. J. Transitioning towards asymmetric gel polymer electrolytes for lithium batteries: progress and prospects. *Adv. Funct. Mater.* **2024**, *34*, 2311215.
[12] An, Y.;Han, X.;Liu, Y.;Azhar, A.;Na, J.;Nanjundan, A. K.;Wang, S.;Yu, J.; Yamauchi, Y. Progress in solid polymer electrolytes for lithium‐ion batteries and beyond. *Small* **2022**, *18*, 2103617.
[13] Marchiori, C. F.;Carvalho, R. P.;Ebadi, M.;Brandell, D.; Araujo, C. M. Understanding the electrochemical stability window of polymer electrolytes in solid-state batteries from atomic-scale modeling: the role of Li-ion salts. *Chem. Mater.* **2020**, *32*, 7237–7246.
[14] Huang, Z.;Fan, H.;Jiang, G.;Xiong, J.; Yuan, S. Facing the ionic conductivity of solid polymer electrolytes for sodium–metal batteries: a mini review. *ACS Appl. Mater. Interfaces* **2025**, *17*, 34915–34930.
[15] Zhu, M.;Wu, J.;Wang, Y.;Song, M.;Long, L.;Siyal, S. H.;Yang, X.; Sui, G. Recent advances in gel polymer electrolyte for high-performance lithium batteries. *J. Energy Chem.* **2019**, *37*, 126–142.
[16] Fan, L.;Wei, S.;Li, S.;Li, Q.; Lu, Y. Recent progress of the solid‐state electrolytes for high‐energy metal‐based batteries. *Adv. Energy Mater.* **2018**, *8*, 1702657.
[17] Sun, C.;Liu, J.;Gong, Y.;Wilkinson, D. P.; Zhang, J. Recent advances in all-solid-state rechargeable lithium batteries. *Nano Energy* **2017**, *33*, 363–386.
[18] Zhong, Q.;Liu, B.;Yang, B.;Li, Y.;Li, J.; Yan, X. Flexible lithium metal capacitors enabled by an in situ prepared gel polymer electrolyte. *Chin. Chem. Lett.* **2021**, *32*, 3496–3500.
[19] Yang, W.;Yang, W.;Zou, R.;Huang, Y.;Lai, H.;Chen, Z.; Peng, X. Cellulose nanofiber‐derived carbon aerogel for advanced room‐temperature sodium–sulfur batteries. *Carbon Energy* **2023**, *5*, e203.
[20] Xu, C.;Li, B.;Du, H.; Kang, F. Energetic zinc ion chemistry: the rechargeable zinc ion battery. *Angew. Chem. Inter. Ed.* **2012**, *51*, 933–935.
[21] Wu, X.;Xu, Y.;Zhang, C.;Leonard, D. P.;Markir, A.;Lu, J.; Ji, X. Reverse dual-ion battery via a ZnCl2 water-in-salt electrolyte. *J. Am. Chem. Soc.* **2019**, *141*, 6338–6344.
[22] Li, J.;Yu, P.;Zhang, S.;Wen, Z.;Wen, Y.;Zhou, W.;Dong, X.;Liu, Y.; Liang, Y. Mild synthesis of superadhesive hydrogel electrolyte with low interfacial resistance and enhanced ionic conductivity for flexible zinc ion battery. *J. Colloid Interface Sci.* **2021**, *600*, 586–593.
[23] He, Q.;Fang, G.;Chang, Z.;Zhang, Y.;Zhou, S.;Zhou, M.;Chai, S.;Zhong, Y.;Cao, G.; Liang, S. Building ultra-stable and low-polarization composite Zn anode interface via hydrated polyzwitterionic electrolyte construction. *Nano-Micro Lett.* **2022**, *14*, 93.

Just Accepted

[24] Xiao, X.;Guo, F.;Mi, H.;Chang, X.;Yin, H.;Ji, C.; Qiu, J. Controlling dendrite growth with xylan-enhanced hydroxyl-rich hydrogel electrolyte for efficient zn-ion energy storage. *ACS Sustain. Chem. Eng.* **2023**, *12*, 470–479.
[25] Zhang, J.;Lin, C.;Zeng, L.;Lin, H.;He, L.;Xiao, F.;Luo, L.;Xiong, P.;Yang, X.; Chen, Q. A Hydrogel Electrolyte with High Adaptability over a Wide Temperature Range and Mechanical Stress for Long‐Life Flexible Zinc‐Ion Batteries. *Small* **2024**, *20*, 2312116.
[26] Zhou, J.;Lu, X.;Li, C.;Zhang, T.;Li, T.;Wu, X.;He, Y.;Zhao, H.;Zhou, H.; Liu, H. Bioimplantable and bioresorbable zinc-ion batteries based on biomacromolecule hydrogel electrolytes. *Chem. Eng. J.* **2025**, *519*, 164927.
[27] Miao, R.;Fan, X.;Zhang, N.;Gao, M.;Mao, Y.; Li, Y. Fabrication of Antifreezing and Adhesive Hydrogel Electrolytes Based on Zwitterionic Proline for Flexible Zinc Ion Batteries with Low-Temperature Tolerance. *ACS Sustain. Chem. Eng.* **2026**.
[28] Cho, Y. G.;Hwang, C.;Cheong, D. S.;Kim, Y. S.; Song, H. K. Gel/solid polymer electrolytes characterized by in situ gelation or polymerization for electrochemical energy systems. *Adv. Mater.* **2019**, *31*, 1804909.
[29] Tripathi, M.;Bobade, S. M.; Kumar, A. Preparation of polyvinylidene fluoride-co-hexafluoropropylene-based polymer gel electrolyte and its performance evaluation for application in EDLCs. *ACS Sustain. Chem. Eng.* **2019**, *42*, 27.
[30] Zou, T.;Jiang, B.;Qu, Q.;Cao, B.;Xu, J.;Zhen, S.;Zhang, J.;Ling, L.;Lu, Y.; Zhang, T. Tea Polyphenol-Derived Zinc-Rich Complexes for Enhanced Interfacial Dynamics in PEO-Based Gel Electrolytes. *ACS Appl. Mater. Interfaces* **2025**, *17*, 13725–13735.
[31] Poompiew, N.;Jirawatanaporn, N.;Okhawilai, M.;Qin, J.;Román, A. J.;Aumnate, C.;Osswald, T. A.; Potiyaraj, P. 3D-printed polyacrylamide-based hydrogel polymer electrolytes for flexible zinc-ion battery. *Electrochim. Acta* **2023**, *466*, 143076.
[32] Wu, K.;Huang, J.;Yi, J.;Liu, X.;Liu, Y.;Wang, Y.;Zhang, J.; Xia, Y. Recent advances in polymer electrolytes for zinc ion batteries: mechanisms, properties, and perspectives. *Adv. Energy Mater.* **2020**, *10*, 1903977.
[33] Vandeginste, V.; Wang, J. A review of the synthesis of biopolymer hydrogel electrolytes for improved electrode–electrolyte interfaces in zinc-ion batteries. *Energies* **2024**, *17*, 310.
[34] Chang, L.;Li, J.;Sun, Q.;Liu, X.;Lu, X.; Cheng, H. Innovative zinc anodes: advancing metallurgy methods to battery applications. *Small* **2024**, *20*, 2408124.
[35] Wan, F.;Zhou, X.;Lu, Y.;Niu, Z.; Chen, J. Energy storage chemistry in aqueous zinc metal batteries. *ACS Energy Lett.* **2020**, *5*, 3569–3590.
[36] Yang, Y.;Tang, Z.;Bian, S.;Gu, Y.;Ye, F.;Chen, W.;Zhu, K.;Wu, Y.; Hu, L. Zinc ion transport kinetics in zinc‐based batteries and its regulation strategy. *Adv. Energy Mater.* **2025**, *15*, 2500316.
[37] Jiang, Y.;Wan, Z.;He, X.; Yang, J. Fine‐Tuning electrolyte concentration and metal–organic framework surface toward actuating fast Zn2+ dehydration for aqueous Zn‐ion batteries. *Angew. Chem. Int. Ed.* **2023**, *62*, e202307274.
[38] Sui, Y.; Ji, X. Anticatalytic strategies to suppress water electrolysis in aqueous batteries. *Chem. Rev.* **2021**, *121*, 6654–6695.
[39] Shang, Y.;Tong, Z.; Kundu, D. Decoding the zinc depletion-mediated failure in aqueous zinc batteries: on limiting parameters and accurate assessment. *ACS Energy Lett.* **2024**, *9*, 3084–3092.
[40] Nian, Q.;Zhang, X.;Feng, Y.;Liu, S.;Sun, T.;Zheng, S.;Ren, X.;Tao, Z.;Zhang, D.; Chen, J. Designing electrolyte structure to suppress hydrogen evolution reaction in aqueous batteries. *ACS Energy Lett.* **2021**, *6*, 2174–2180.

Just Accepted

[41] Li, B.;Ma, Y.;Ma, J.;Chen, L.;Zhao, Y.; Tang, M.-C. Challenges and opportunities facing zinc anodes for aqueous zinc-ion battery. *Energy Mater. Devices* **2024**, *2*, 9370044.
[42] Sharma, P.; Banerjee, D. Biopolymers as solid polymer electrolytes: advances, challenges, and future prospects. *Prabha Mater Sci Lett* **2025**, *4*, 128–147.
[43] Fuzlin, A.;Aynharan, S.;Hafidz, N.;Ghazali, N.;Diantoro, M.;Nagao, Y.; Samsudin, A. Advances in gel biopolymer electrolytes: sustainable polymers for energy storage applications. *Polym. Adv. Technol.* **2025**, *36*, e70319.
[44] Martinez-Ibanez, M.;Boaretto, N.;Meabe, L.;Wang, X.;Zhu, H.;Santiago, A.;Zugazua, O.;Forsyth, M.;Armand, M.; Zhang, H. Revealing the anion chemistry effect on transport properties of ternary gel polymer electrolytes. *Chem. Mater.* **2022**, *34*, 7493–7502.
[45] Jain, A.;Mahata, K.;Onkarnath; Banerjee, S. Biopolymer Derived Gel Polymer Electrolytes: Current Status and Future Perspectives. *Macromol. Rapid Commun.* **2025**, e00472.
[46] Shan, Y.;Lu, B.;Li, T.;Zang, B.;Huang, H.;Yuan, Q.;Zou, Y.;Qiu, S.;Yin, X.; Ren, Y. Mechanically and Thermally Robust Gel Polymer Electrolytes with Dynamic Hydrogen-Bond Networks for Wide-Temperature Lithium Metal Batteries. *ACS Appl. Mater. Interfaces* **2025**, *17*, 57191–57203.
[47] Wu, M.;Zhang, Y.;Xu, L.;Yang, C.;Hong, M.;Cui, M.;Clifford, B. C.;He, S.;Jing, S.; Yao, Y. A sustainable chitosan-zinc electrolyte for high-rate zinc-metal batteries. *Matter* **2022**, *5*, 3402–3416.
[48] Xu, L.;Meng, T.;Zheng, X.;Li, T.;Brozena, A. H.;Mao, Y.;Zhang, Q.;Clifford, B. C.;Rao, J.; Hu, L. Nanocellulose‐carboxymethylcellulose electrolyte for stable, high‐rate zinc‐ion batteries. *Adv. Funct. Mater.* **2023**, *33*, 2302098.
[49] Niazi, M.;Danzi, F.; Camanho, P. P. Trade-offs between load-bearing capability and ionic conductivity of composite polymer electrolytes. *Compos. Struct.* **2025**, 119875.
[50] Ren, Z.;Wang, Y.;Ye, Q.;Ye, F.;Kang, R.;Wang, H.;Zhang, X.;Zhang, B.;Zhai, J.; Zhang, J. Tailored Inorganic Fillers in Composite Solid‐State Electrolytes: Enabling Synergistic Enhancement of Ionic Conduction and Interfacial Stability for High‐Performance ASSLBs. *Small* **2025**, *21*, e08824.
[51] Zhu, L.;Yang, H.;Liu, K.;Li, W.;Tang, Y.;Li, X.;Xu, T.;Dai, L.; Si, C. Molecularly engineered cellulose: the next-generation sustainable polymer electrolyte material. *Energy Environ. Sci.* **2026**, *19*, 1407–1457.
[52] Appel, E. A.;del Barrio, J.;Loh, X. J.; Scherman, O. A. Supramolecular polymeric hydrogels. *Chem. Soc. Rev.* **2012**, *41*, 6195–6214.
[53] Pruksawan, S.;Chong, Y. T.;Lee, Y. S. Y.;Lam, D. K. F.; Wang, F. Design strategies and perspectives on the toughening of hydrogels via fully physical cross-linking. *Chem. Mater.* **2025**, *37*, 5436–5453.
[54] Aruchamy, K.;Ramasundaram, S.;Divya, S.;Chandran, M.;Yun, K.; Oh, T. H. Gel polymer electrolytes: advancing solid-state batteries for high-performance applications. *Gels* **2023**, *9*, 585.
[55] Jebin, P.;Khan, M. R.;Shah, S. S.;Debnath, N.;Aziz, M. A.;Kim, B. J.; Ahammad, A. S. Synergistic Integration of Quantum Materials with Smart Electrolytes for Next‐Generation Multifunctional Supercapacitors: Advances, Challenges, and Future Prospects. *Small* **2026**, *22*, e08559.
[56] Wang, Z.;Li, H.;Tang, Z.;Liu, Z.;Ruan, Z.;Ma, L.;Yang, Q.;Wang, D.; Zhi, C. Hydrogel electrolytes for flexible aqueous energy storage devices. *Adv. Funct. Mater.* **2018**, *28*, 1804560.

Just Accepted

[57] Chan, C. Y.;Wang, Z.;Jia, H.;Ng, P. F.;Chow, L.; Fei, B. Recent advances of hydrogel electrolytes in flexible energy storage devices. *J. Mater. Chem. A* **2021**, *9*, 2043–2069.
[58] Du, Z.;Shen, S.;Su, X.;Zhuang, Y.;Chen, M.;Zhang, X.;Lin, Z.;Yu, L.;Zhou, P.; Wu, M. A Robust and Tough Composite Hydrogel Electrolyte with Anion‐Locked Supramolecular Network for Zinc Ion Batteries. *Adv. Mater.* **2025**, *37*, 2502328.
[59] Tariq, Z.;Iqbal, D. N.;Rizwan, M.;Ahmad, M.;Faheem, M.; Ahmed, M. Significance of biopolymer-based hydrogels and their applications in agriculture: a review in perspective of synthesis and their degree of swelling for water holding. *RSC advances* **2023**, *13*, 24731–24754.
[60] Radjendirane, A. C.;Sha, F. M.;Ramasamy, S.;Rajaram, R.; Angaiah, S. A Review on Recent Advances and Perspectives in Hydrogel Polymer Electrolytes for Aqueous Zinc‐Ion Batteries. *Energy Technol.* **2024**, *12*, 2401105.
[61] Ma, R.;Xu, Z.; Wang, X. Polymer hydrogel electrolytes for flexible and multifunctional zinc‐ion batteries and capacitors. *Energy Environ. Mater.* **2023**, *6*, e12464.
[62] Akhter, Z.;Ullah, S.;Palevicius, A.; Janusas, G. Agar-based composites in sustainable energy storage: a comprehensive review. *Energies* **2025**, *18*, 5618.
[63] Li, S.;Wang, Q.;Wang, J.;Jiang, H.; Du, F. Comprehensive insights into gel polymer electrolytes and electrode/electrolyte Interfaces for aqueous Zinc ion batteries. *ChemSusChem* **2025**, *18*, e202500942.
[64] Fan, M.;Lv, L.;Xue, S.;Yan, D.;Ma, G.;Wang, H.;Wan, H.; Wang, H. Emerging Advanced Design Strategies and Engineering toward Polymer‐Hydrogel Electrolytes for Flexible Zinc‐Based Rechargeable Batteries: A Review From an All‐Around Insight. *Small* **2025**, *21*, 2505804.
[65] Liu, C.;Xie, X.;Lu, B.;Zhou, J.; Liang, S. Electrolyte strategies toward better zinc-ion batteries. *ACS Energy Lett.* **2021**, *6*, 1015–1033.
[66] Huang, S.;Hou, L.;Li, T.;Jiao, Y.; Wu, P. Antifreezing hydrogel electrolyte with ternary hydrogen bonding for high‐performance zinc‐ion batteries. *Adv. Mater.* **2022**, *34*, 2110140.
[67] Li, X.;Wang, H.;Sun, X.;Li, J.; Liu, Y.-N. Flexible wide-temperature zinc-ion battery enabled by an ethylene glycol-based organohydrogel electrolyte. *ACS Appl. Energy Mater.* **2021**, *4*, 12718–12727.
[68] Zhang, X.;Yu, Q.;Qu, G.;Wang, X.;Li, C.;Wang, C.;Li, N.;Huang, J.;Han, C.; Li, H. Synergistic enhancement of cathode/anode interfaces with high water-retentive organohydrogel enabling highly stable zinc ion batteries. *J. Energy Chem.* **2024**, *98*, 670–679.
[69] Chen, Y.;Zhu, M.;Li, C.;Wang, H.;Chen, D.;Wu, H.;Huang, Z.;Wang, Y.;Fan, Y.; Bai, Z. Ionic liquid‐based hydrogel electrolytes enabling high‐voltage‐plateau zinc‐ion batteries. *Adv. Funct. Mater.* **2025**, *35*, 2501162.
[70] Liu, J.;Nie, N.;Wang, J.;Hu, M.;Zhang, J.;Li, M.; Huang, Y. Initiating a wide-temperature-window yarn zinc ion battery by a highly conductive iongel. *Mater. Today Energy* **2020**, *16*, 100372.
[71] Qi, R.;Tang, W.;Shi, Y.;Teng, K.;Deng, Y.;Zhang, L.;Zhang, J.; Liu, R. Gel polymer electrolyte toward large‐scale application of aqueous zinc batteries. *Adv. Funct. Mater.* **2023**, *33*, 2306052.
[72] Li, J.;Zhang, H.;Liu, Z.;Du, H.;Wan, H.;Li, X.;Yang, J.; Yan, C. Boosting dendrite‐free zinc anode with strongly polar functional group terminated hydrogel electrolyte for high‐safe aqueous zinc‐ion batteries. *Adv. Funct. Mater.* **2025**, *35*, 2412865.

Just Accepted

[73] Kao‐ian, W.;Mohamad, A. A.;Liu, W. R.;Pornprasertsuk, R.;Siwamogsatham, S.; Kheawhom, S. Stability enhancement of zinc‐ion batteries using non‐aqueous electrolytes. *Batter. Supercaps* **2022**, *5*, e202100361.
[74] Cao, J.;Zhao, F.;Guan, W.;Yang, X.;Zhao, Q.;Gao, L.;Ren, X.;Wu, G.; Liu, A. Additives for Aqueous Zinc‐Ion Batteries: Recent Progress, Mechanism Analysis, and Future Perspectives. *Small* **2024**, *20*, 2400221.
[75] Fu, M.;Zhao, Q.;Long, K.;Li, Q.;Kuang, G. c.;Zhou, L.;Wei, W.;Ji, X.;Chen, L.; Chen, Y. Global "interface‐space" dual‐modulation by functional supramolecules organic frameworks on aqueous zinc‐ion batteries. *Adv. Funct. Mater.* **2024**, *34*, 2311680.
[76] Wang, W.;Yue, X.;Liang, Z.;Liu, X.;Wang, D.;Zhou, H.;Yu, J.; Yang, G. Recent progress in hydrogel electrolytes for advanced flexible zinc-ion batteries. *Discover Electrochemistry* **2026**, *3*, 4.
[77] Bósquez-Cáceres, M. F.;Hidalgo-Bonilla, S.;Morera Córdova, V.;Michell, R. M.; Tafur, J. P. Nanocomposite polymer electrolytes for zinc and magnesium batteries: from synthetic to biopolymers. *Polymers* **2021**, *13*, 4284.
[78] Chen, M.;Cheng, J.;Zhao, Y.;Fu, W.;Li, W.;Zhu, Y.; Meng, F. Ion-Sieving Dual-Network Hydrogel Electrolytes Couple Accelerated Ion Transport with Iodide Shuttle Suppression in Aqueous Zn–I2 Batteries. *Nano-Micro Lett.* **2026**, *18*, 366.
[79] Nie, C.;Wang, G.;Wang, D.;Wang, M.;Gao, X.;Bai, Z.;Wang, N.;Yang, J.;Xing, Z.; Dou, S. Recent progress on Zn anodes for advanced aqueous zinc‐ion batteries. *Adv. Energy Mater.* **2023**, *13*, 2300606.
[80] Liu, J.;Khanam, Z.;Ahmed, S.;Wang, T.;Wang, H.; Song, S. Flexible antifreeze Zn-ion hybrid supercapacitor based on gel electrolyte with graphene electrodes. *ACS Appl. Mater. Interfaces* **2021**, *13*, 16454–16468.
[81] Singh, S. B.;Tran, D. T.;Jeong, K. U.;Kim, N. H.; Lee, J. H. A flexible and transparent zinc‐nanofiber network electrode for wearable electrochromic, rechargeable Zn‐ion battery. *Small* **2022**, *18*, 2104462.
[82] Dong, H.;Li, J.;Guo, J.;Lai, F.;Zhao, F.;Jiao, Y.;Brett, D. J.;Liu, T.;He, G.; Parkin, I. P. Insights on flexible zinc‐ion batteries from lab research to commercialization. *Adv. Mater.* **2021**, *33*, 2007548.
[83] Yin, J.-J.;Li, Y.;Sun, X.; Qin, Z.-H. Tough gelatin-based biogels for wearable sensors. *Soft Sci.* **2025**, *5*, N/A–N/A.
[84] Zhang, S.-y.;Li, Y.-r.;Xing, T.;Liu, H.-y.;Liu, Z.-b.;Li, Z.-t.; Wu, M.-b. Recent progress in the use of polyanions as solid electrolytes. *New Carbon Mater.* **2022**, *37*, 358–370.
[85] Ye, J.-C.;Lai, Y.-W.;Huang, X.-H.;Chang, Z.-X.;Chung, Y.-H.; Shu, C.-M. Development of the electrolyte in lithium-ion battery: a concise review on its thermal hazards. *J. Therm. Anal. Calorim.* **2024**, *149*, 11293–11312.
[86] Baek, J.;Shin, A.;Kim, N.;Lee, S.-H.; Kim, B.-S. Topology-Controlled Polyethers: A Synthetic Platform for Tunable Properties and Applications. *Acc. Mater. Res.* **2025**, *6*, 1204–1219.
[87] Barman, R.; Lutz, J.-F. A general strategy to access all stereosequences in a synthetic polymer. *J. Am. Chem. Soc.* **2025**, *147*, 44430–44436.
[88] Erothu, H.; Kumar, A. C. Hydrophilic polymers. *Biomedical applications of polymeric materials and composites* **2016**, 163–185.
[89] Ahmed, A.;Subchokpool, T.;Khampuanbut, A.;Hongrattanavichit, I.;Okhawilai, M.;Sukmas, W.; Pattananuwat, P. Enhancing high ionic conductivity of polyacryamide/hemp cellulose nanofibers for utilizing as quasi solid electrolyte

JSB Accepted

composites in flexible rechargeable zinc-ion battery with high-safety. *Mater. Today Sustain.* **2025**, *30*, 101088.
[90] Niu, B.;Wang, J.;Guo, Y.;Li, Z.;Yuan, C.;Ju, A.; Wang, X. Polymers for aqueous zinc‐ion batteries: from fundamental to applications across core components. *Adv. Energy Mater.* **2024**, *14*, 2303967.
[91] Puthiyaveetil, P. P.;Kurian, R. M.;Samudre, N. S.;Balasubramanian, R.;Torris, A.;Pockil, F. K.;Bhat, S.;Ajithkumar, T.;Krishnamurty, S.; Kurungot, S. Self‐Healing Hydrogel Electrolyte Enabled by Dynamic Polar Covalent and Noncovalent Interactions for High‐Performance Rechargeable Zinc‐Metal Batteries: A Leap Toward Sustainable Energy Storage. *Adv. Energy Mater.* **2026**, *16*, e02883.
[92] Arif, M.;Yang, L.;Zhang, Q.; Wang, H. Mechanistic Perspectives: Integration and Repairing Adaptation of Self‐Healing Electrolytes for Zinc Ion Batteries. *Batter. Supercaps* **2024**, *7*, e202400487.
[93] Huang, S.;Wan, F.;Bi, S.;Zhu, J.;Niu, Z.; Chen, J. A self‐healing integrated all‐in‐one zinc‐ion battery. *Angew. Chem.* **2019**, *131*, 4357–4361.
[94] Li, S.;Liu, Y.;Zhao, X.;Cui, K.;Shen, Q.;Li, P.;Qu, X.; Jiao, L. Molecular engineering on MoS2 enables large interlayers and unlocked basal planes for high‐performance aqueous Zn‐ion storage. *Angew. Chem.* **2021**, *133*, 20448–20455.
[95] Ouyang, K.;Li, F.;Ma, D.;Wang, Y.;Shen, S.;Yang, M.;Qiu, J.;Wen, W.;Zhao, N.; Mi, H. Trace-additive-mediated hydrophobic structure editing of aqueous zinc metal batteries for enabling all-climate long-term operation. *ACS Energy Lett.* **2023**, *8*, 5229–5239.
[96] Zhang, X.;Pei, Z.;Wang, C.;Yuan, Z.;Wei, L.;Pan, Y.;Mahmood, A.;Shao, Q.; Chen, Y. Flexible zinc‐ion hybrid fiber capacitors with ultrahigh energy density and long cycling life for wearable electronics. *Small* **2019**, *15*, 1903817.
[97] Zia, F.;Anjum, M. N.;Saif, M. J.;Jamil, T.;Malik, K.;Anjum, S.;BiBi, I.; Zia, M. A. Alginate-poly (ethylene) glycol and poly (ethylene) oxide blend materials. In *Algae based polymers, blends, and composites*. Elsevier, 2017; pp 581–601.
[98] Wang, D.;Guo, X.;Chen, Z.;Zhao, Y.;Li, Q.; Zhi, C. Ionic liquid-softened polymer electrolyte for anti-drying flexible zinc ion batteries. *ACS Appl. Mater. Interfaces* **2022**, *14*, 27287–27293.
[99] Liu, X.;Li, X.;Yang, X.;Lu, J.;Zhang, X.;Yuan, D.; Zhang, Y. Influence of Water on Gel Electrolytes for Zinc‐Ion Batteries. *Chem. Asian J.* **2023**, *18*, e202201280.
[100] Wu, Q.;Huang, J.;Zhang, J.;Yang, S.;Li, Y.;Luo, F.;You, Y.;Li, Y.;Xie, H.; Chen, Y. Multifunctional Cellulose Nanocrystals Electrolyte Additive Enable Ultrahigh‐Rate and Dendrite‐Free Zn Anodes for Rechargeable Aqueous Zinc Batteries. *Angew. Chem. Int. Ed.* **2024**, *63*, e202319051.
[101] Zhang, B.;Qin, L.;Fang, Y.;Chai, Y.;Xie, X.;Lu, B.;Liang, S.; Zhou, J. Tuning Zn2+ coordination tunnel by hierarchical gel electrolyte for dendrite-free zinc anode. *Sci. Bull.* **2022**, *67*, 955–962.
[102] Zhao, X.;Huang, S.;Tang, Z.;Liu, D.;Xie, C.;Yi, X.;Qiu, X.;Chen, H.;Zhu, M.; Zhang, X. Full-Process Proton Management Unlocks Long-Life Aqueous Zinc-Metal Batteries. *ACS nano* **2026**.
[103] Bian, H.;Yu, P.;Li, Z.;Zhang, Y.;Li, Y.;Zhu, X.;Chang, K.;Qin, A.; Zhang, C. Research progress on the application of chitosan in aqueous zinc-ion batteries.
[104] Zhou, H.;He, Q.;Liu, X.;Jiang, Q.;Chu, D.;Wang, Q.;Yang, X.;Zhang, T.;Wang, H.; Li, Z. Cellulose/sodium alginate gel electrolyte membranes with synergistic hydrogen

Just Accepted

bonding and metal ion coordination networks for high performance aqueous zinc-ion batteries. *Carbohydr. Polym.* **2025**, *352*, 123116.
[105] Li, Z.;Zhou, G.;Ye, L.;He, J.;Xu, W.;Hong, S.;Chen, W.;Li, M.-C.;Liu, C.; Mei, C. High-energy and dendrite-free solid-state zinc metal battery enabled by a dual-network and water-confinement hydrogel electrolyte. *Chem. Eng. J.* **2023**, *472*, 144992.
[106] Tu, W. B.;Liang, S.;Song, L. N.;Wang, X. X.;Ji, G. J.; Xu, J. J. Nanoengineered functional cellulose ionic conductor toward high‐performance all‐solid‐state zinc‐ion battery. *Adv. Funct. Mater.* **2024**, *34*, 2316137.
[107] Shang, W.;Zhu, J.;Liu, Y.;Kang, L.;Liu, S.;Huang, B.;Song, J.;Li, X.;Jiang, F.; Du, W. Establishing high-performance quasi-solid Zn/I2 batteries with alginate-based hydrogel electrolytes. *ACS Appl. Mater. Interfaces* **2021**, *13*, 24756–24764.
[108] Lizundia, E.; Kundu, D. Advances in natural biopolymer‐based electrolytes and separators for battery applications. *Adv. Funct. Mater.* **2021**, *31*, 2005646.
[109] Li, Z.;Qiu, C.;Zhang, H.;Zhang, W.;Zhu, C.;Lan, W.;Ji, Z.;Zhang, Y.;Tian, W.; Chen, J. High‐Efficiency Flexible Zn‐Air Batteries Enabled by Agarose Based Oxygen Electrocatalyst and Gel Electrolyte Through Bidirectionally Synergistic Optimization Strategy. *Small Methods* **2026**, *10*, 2500877.
[110] Kumankuma‐Sarpong, J.;Chang, C.;Hao, J.;Li, T.;Deng, X.;Han, C.; Li, B. Entanglement added to cross‐linked chains enables tough gelatin‐based hydrogel for Zn metal batteries. *Adv. Mater.* **2024**, *36*, 2403214.
[111] Zhang, S.;Yu, N.;Zeng, S.;Zhou, S.;Chen, M.;Di, J.; Li, Q. An adaptive and stable bio-electrolyte for rechargeable Zn-ion batteries. *J. Mater. Chem. A* **2018**, *6*, 12237–12243.
[112] Wang, H.;Wang, W.; Xie, Z. Patterning meets gels: Advances in engineering functional gels at micro/nanoscales for soft devices. *J. Polym. Sci.* **2022**, *60*, 2679–2700.
[113] Feng, Y.;Yu, J.;Shao, C.; Sun, R. Advances toward sustainable lignin-based gel for energy storage and smart sensing. *Pap. Biomater* **2023**, *8*, 20–36.
[114] Lorca, S.;Santos, F.; Fernandez Romero, A. J. A review of the use of GPEs in zinc-based batteries. A step closer to wearable electronic gadgets and smart textiles. *Polymers* **2020**, *12*, 2812.
[115] Belza, B.;Palermo, M. F.;García-Gaitán, E.;de Larramendi, I. R.; Ortiz-Vitoriano, N. Biopolymer Electrolytes for Rechargeable Zinc-Air Batteries: Advancements and Challenges. *Curr. Opin. Electrochem.* **2026**, 101821.
[116] Feng, Y. Research Progress on Modification and Functionalization of Gel Electrolyte for Aqueous Zinc Ion Batteries.
[117] Li, S.; Zhi, C. Versatile biopolymers for advanced lithium and zinc metal batteries. *Adv. Mater.* **2025**, *37*, 2413515.
[118] Abbasi, A.;Xu, Y.;Abouzari-Lotf, E.;Etesami, M.;Khezri, R.;Risse, S.;Kardjilov, N.;Van Tran, K.;Jia, H.; Somwangthanaroj, A. Phosphonated graphene oxide-modified polyacrylamide hydrogel electrolytes for solid-state zinc-ion batteries. *Electrochim. Acta.* **2022**, *435*, 141365.
[119] De Cachinho Cordeiro, I. M.;Li, A.;Lin, B.;Ma, D. X.;Xu, L.;Eh, A. L.-S.; Wang, W. Solid polymer electrolytes for zinc-ion batteries. *Batteries* **2023**, *9*, 343.
[120] Wang, Y.;Jiang, Z.;Yang, Q.;He, Q.;Zarifzoda, A. Q.; Chen, F. Ethanolamine-modified gel electrolyte of zinc ion battery. *J. Alloys Compd.* **2025**, *1010*, 177192.

JES Accepted

[121] Rajabi, R.;Sun, S.;Wu, B.;Khan, J.; Huang, K. Towards Sustainable Energy Storage: Evaluating the Performance of Three Polymer Electrolytes for Zinc-Ion Batteries. *Batteries* **2026**, *12*, 93.
[122] Panteli, P. A.; Patrickios, C. S. Multiply interpenetrating polymer networks: Preparation, mechanical properties, and applications. *Gels* **2019**, *5*, 36.
[123] Zeng, W.;Zhang, S.;Lan, J.;Lv, Y.;Zhu, G.;Huang, H.;Lv, W.; Zhu, Y. Double network gel electrolyte with high ionic conductivity and mechanical strength for zinc-ion batteries. *ACS nano* **2024**, *18*, 26391–26400.
[124] Tan, H.;Meng, C.;Chen, H.;Yang, J. L.;Cao, J. M.;Wu, X. L.; Wang, J. J. Breaking the ice: hofmeister effect‐inspired hydrogen bond network reconstruction in hydrogel electrolytes for high‐performance zinc‐ion batteries. *Small* **2025**, *21*, 2410746.
[125] Chen, G.;Zhuang, W.; Mekonnen, T. Biomass-derived materials for next-generation solid-state batteries: From sustainable resources to advanced electrodes and electrolytes. *ENGIN. Energy* **2026**, *20*, 10789.
[126] Jia, R.;Wei, C.;Ma, B.;Li, L.;Yang, C.;Wang, B.;Tan, L.; Feng, J. Biopolymer‐based gel electrolytes for advanced zinc ion batteries: progress and perspectives. *Adv. Funct. Mater.* **2025**, *35*, 2417498.
[127] Sun, L.;Yao, Y.;Dai, L.;Jiao, M.;Ding, B.;Yu, Q.;Tang, J.; Liu, B. Sustainable and high-performance Zn dual-ion batteries with a hydrogel-based water-in-salt electrolyte. *Energy Storage Mater.* **2022**, *47*, 187–194.
[128] Tan, H.;Wu, X.-L.; Wang, J.-J. Dynamic Noncovalent Interactions: The Role of Supramolecular Chemistry in Stabilizing Aqueous Zinc-Ion Batteries. *Acc. Chem. Res.* **2026**, *59*, 1879–1892.
[129] Yang, C.;Woottapanit, P.;Geng, S.;Chanajaree, R.;Shen, Y.;Lolupiman, K.;Limphirat, W.;Pakornchote, T.;Bovornratanaraks, T.; Zhang, X. A multifunctional quasi-solid-state polymer electrolyte with highly selective ion highways for practical zinc ion batteries. *Nat. Commun.* **2025**, *16*, 183.
[130] Wang, Z.;Xue, R.;Zhang, H.;Zhang, Y.;Tang, X.;Wang, H.;Shao, A.; Ma, Y. A hydrogel electrolyte toward a flexible zinc-ion battery and multifunctional health monitoring electronics. *ACS nano* **2024**, *18*, 7596–7609.
[131] Wang, D.;Li, H.;Liu, Z.;Tang, Z.;Liang, G.;Mo, F.;Yang, Q.;Ma, L.; Zhi, C. A nanofibrillated cellulose/polyacrylamide electrolyte‐based flexible and sewable high‐performance Zn–MnO2 battery with superior shear resistance. *Small* **2018**, *14*, 1803978.
[132] Tong, C.;Chen, Y.;Janssen, M. L.;Sariol, I.;Wondergem, J. A.;den Brink, M. v.;Özel, M.;Nelissen, R. G.;Meulenbelt, I.; Heinrich, D. Supramolecular Engineering of Fluid Pressure in Filamentous Hybrid Double Network Hydrogels for 3D Chondrocyte Culture. *Adv. Healthc. Mater.* **2026**, *15*, e05238.
[133] Takahashi, R.;Ikai, T.;Kurokawa, T.;King, D. R.; Gong, J. P. Double network hydrogels based on semi-rigid polyelectrolyte physical networks. *J. Mater. Chem. B* **2019**, *7*, 6347–6354.
[134] Zhang, B.;Gao, Z.;Gao, G.;Zhao, W.;Li, J.; Ren, X. Highly Mechanical and Fatigue‐Resistant Double Network Hydrogels by Dual Physically Hydrophobic Association and Ionic Crosslinking. *Macromol. Mater. Eng.* **2018**, *303*, 1800072.
[135] Yao, L.;Liu, J.;Zhang, F.;Wen, B.;Chi, X.; Liu, Y. Reconstruction of zinc-metal battery solvation structures operating from− 50~+ 100° C. *Nat. Commun.* **2024**, *15*, 6249.

Just Accepted

[136] Lin, D.;Lin, Y.;Pan, R.;Li, J.;Zhu, A.;Zhang, T.;Liu, K.;Feng, D.;Liu, K.; Zhou, Y. Water-restrained hydrogel electrolytes with repulsion-driven cationic express pathways for durable zinc-ion batteries. *Nano-Micro Lett.* **2025**, *17*, 193.
[137] Zhang, H.;Gan, X.;Yan, Y.; Zhou, J. A sustainable dual cross-linked cellulose hydrogel electrolyte for high-performance zinc-metal batteries. *Nano-Micro Lett.* **2024**, *16*, 106.
[138] Li, D.;Zhong, Y.;Wan, C.;Lu, B.;Liu, Y.; Zhou, J. Strain-resilient zinc-ion batteries enabled by mechanical-ionic coupled dissipation in hydrogel electrolyte. *Matter* **2026**.
[139] Chen, D.;Wang, C.;Yu, Y.;Ren, Z.; Zhao, R. Dynamic hydrogen-bond-driven thorium ion traps in sodium alginate/tannic acid beads. *J. Hazard. Mater.* **2026**, *506*, 141672.
[140] Zhao, C.;Zhang, Y.;Gao, J.;Guo, Z.;Chen, A.;Liu, N.;Lu, X.;Zhang, X.; Zhang, N. Zincophilic Design and the Electrode/Electrolyte Interface for Aqueous Zinc‐Ion Batteries: A Review. *Batter. Supercaps* **2023**, *6*, e202200478.
[141] Zhao, S.;Zuo, Y.;Liu, T.;Zhai, S.;Dai, Y.;Guo, Z.;Wang, Y.;He, Q.;Xia, L.; Zhi, C. Multi‐functional hydrogels for flexible zinc‐based batteries working under extreme conditions. *Adv. Energy Mater.* **2021**, *11*, 2101749.
[142] Fu, C.;Wang, Y.;Lu, C.;Zhou, S.;He, Q.;Hu, Y.;Feng, M.;Wan, Y.;Lin, J.; Zhang, Y. Modulation of hydrogel electrolyte enabling stable zinc metal anode. *Energy Storage Mater.* **2022**, *51*, 588–598.
[143] Sun, Y.;Song, L. N.;Du, X. Y.;Liang, S.;Wang, Y.;Wang, X. X.;Ji, G. J.; Xu, J. J. In Situ Copolymerizing ZrO2 with Hydrogel Electrolytes toward High‐Rate and Long‐Life Quasi‐Solid‐State Zn–Ion Batteries. *Adv. Energy Mater.* **2025**, *15*, 2404944.
[144] Chen, Q.;Zhu, L.;Chen, H.;Yan, H.;Huang, L.;Yang, J.; Zheng, J. A novel design strategy for fully physically linked double network hydrogels with tough, fatigue resistant, and self‐healing properties. *Adv. Funct. Mater.* **2015**, *25*, 1598–1607.
[145] Lin, Y.;Wang, S.;Huang, J.;Chen, L.;Bi, T.;Qi, L.;Cai, Z.;Zeng, X.;Hu, P.; Chen, W. Coupling of mechanical, self‐healing, adhesion, and high‐ion conducting properties in anti‐freezing hydrogel electrolytes of zinc ion batteries via Fe3+‐carboxylate coordination. *Adv. Funct. Mater.* **2025**, *35*, 2504726.
[146] Cao, L.;Yang, M.;Wu, D.;Lyu, F.;Sun, Z.;Zhong, X.;Pan, H.;Liu, H.; Lu, Z. Biopolymer-chitosan based supramolecular hydrogels as solid state electrolytes for electrochemical energy storage. *Chem. Commun.* **2017**, *53*, 1615–1618.
[147] Kasprzak, D.; Galinski, M. Biopolymer-based gel electrolytes with an ionic liquid for high-voltage electrochemical capacitors. *Available at SSRN 4061365* **2022**.
[148] Wang, J.;Huang, Y.;Liu, B.;Li, Z.;Zhang, J.;Yang, G.;Hiralal, P.;Jin, S.; Zhou, H. Flexible and anti-freezing zinc-ion batteries using a guar-gum/sodium-alginate/ethylene-glycol hydrogel electrolyte. *Energy Storage Mater.* **2021**, *41*, 599–605.
[149] Caldeira, I.;Lüdtke, A.;Tavares, F.;Cholant, C.;Balboni, R.;Flores, W. H.;Galio, A.;Pawlicka, A.; Avellaneda, C. O. Ecologically friendly xanthan gum-PVA matrix for solid polymeric electrolytes. *Ionics* **2018**, *24*, 413–420.
[150] Quan, Y.;Zhou, W.;Wu, T.;Chen, M.;Han, X.;Tian, Q.;Xu, J.; Chen, J. Sorbitol-modified cellulose hydrogel electrolyte derived from wheat straws towards high-performance environmentally adaptive flexible zinc-ion batteries. *Chem. Eng. J.* **2022**, *446*, 137056.
[151] Zhu, M.;Tan, C.;Fang, Q.;Gao, L.;Sui, G.; Yang, X. High performance and biodegradable skeleton material based on soy protein isolate for gel polymer electrolyte. *ACS Sustain. Chem. Eng.* **2016**, *4*, 4498–4505.

Just Accepted

[152] Zhao, N.;Wu, F.;Xing, Y.;Qu, W.;Chen, N.;Shang, Y.;Yan, M.;Li, Y.;Li, L.; Chen, R. Flexible hydrogel electrolyte with superior mechanical properties based on poly (vinyl alcohol) and bacterial cellulose for the solid-state zinc–air batteries. *ACS Appl. Mater. Interfaces* **2019**, *11*, 15537–15542.
[153] Lu, H.;Hu, J.;Wei, X.;Zhang, K.;Xiao, X.;Zhao, J.;Hu, Q.;Yu, J.;Zhou, G.; Xu, B. A recyclable biomass electrolyte towards green zinc-ion batteries. *Nat. Commun.* **2023**, *14*, 4435.
[154] Yang, J.;Weng, C.;Sun, P.;Yin, Y.;Xu, M.;Pan, L.; Li, J. Comprehensive regulation strategies for gel electrolytes in aqueous zinc-ion batteries. *Coord. Chem. Rev.* **2025**, *530*, 216475.
[155] Liu, H.;Ye, Q.;Lei, D.;Hou, Z.;Hua, W.;Huyan, Y.;Li, N.;Wei, C.;Kang, F.; Wang, J.-G. Molecular brush: an ion-redistributor to homogenize fast Zn2+ flux and deposition for calendar-life Zn batteries. *Energy Environ. Sci.* **2023**, *16*, 1610–1619.
[156] Wang, Z.;Hu, J.;Han, L.;Wang, Z.;Wang, H.;Zhao, Q.;Liu, J.; Pan, F. A MOF-based single-ion Zn2+ solid electrolyte leading to dendrite-free rechargeable Zn batteries. *Nano energy* **2019**, *56*, 92–99.
[157] Xia, H.;Xu, G.;Cao, X.;Miao, C.;Zhang, H.;Chen, P.;Zhou, Y.;Zhang, W.; Sun, Z. Single‐ion‐conducting hydrogel electrolytes based on slide‐ring pseudo‐polyrotaxane for ultralong‐cycling flexible zinc‐ion batteries. *Adv. Mater.* **2023**, *35*, 2301996.
[158] Zhang, W.;Guo, F.;Mi, H.;Wu, Z. S.;Ji, C.;Yang, C.; Qiu, J. Kinetics‐boosted effect enabled by zwitterionic hydrogel electrolyte for highly reversible zinc anode in zinc‐ion hybrid micro‐supercapacitors. *Adv. Energy Mater.* **2022**, *12*, 2202219.
[159] Wang, Y.;Chen, F.;Liu, Z.;Tang, Z.;Yang, Q.;Zhao, Y.;Du, S.;Chen, Q.; Zhi, C. A highly elastic and reversibly stretchable all‐polymer supercapacitor. *Ang. Chem.* **2019**, *131*, 15854–15858.
[160] Ma, L.;Chen, S.;Wang, D.;Yang, Q.;Mo, F.;Liang, G.;Li, N.;Zhang, H.;Zapien, J. A.; Zhi, C. Super‐stretchable zinc–air batteries based on an alkaline‐tolerant dual‐network hydrogel electrolyte. *Adv. Energy Mater.* **2019**, *9*, 1803046.
[161] Cao, G.;Zhao, L.;Ji, X.;Peng, Y.;Yu, M.;Wang, X.;Li, X.; Ran, F. "Salting out" in Hofmeister Effect Enhancing Mechanical and Electrochemical Performance of Amide‐based Hydrogel Electrolytes for Flexible Zinc‐Ion Battery. *Small* **2023**, *19*, 2207610.
[162] Zhang, Q.;Hou, X.;Liu, X.;Xie, X.;Duan, L.;Lü, W.; Gao, G. Nucleotide‐tackified organohydrogel electrolyte for environmentally self‐adaptive flexible supercapacitor with robust electrolyte/electrode interface. *Small* **2021**, *17*, 2103091.
[163] Hsu, H. H.;Liu, Y.;Wang, Y.;Li, B.;Luo, G.;Xing, M.; Zhong, W. Mussel-inspired autonomously self-healable all-in-one supercapacitor with biocompatible hydrogel. *ACS Sustain. Chem. Eng.* **2020**, *8*, 6935–6948.
[164] Wu, Z.;Shi, W.;Ding, H.;Zhong, B.;Huang, W.;Zhou, Y.;Gui, X.;Xie, X.; Wu, J. Ultrastable, stretchable, highly conductive and transparent hydrogels enabled by salt-percolation for high-performance temperature and strain sensing. *J. Mater. Chem. C* **2021**, *9*, 13668–13679.
[165] Gu, W.;Li, F.;Liu, T.;Gong, S.;Gao, Q.;Li, J.; Fang, Z. Recyclable, self‐healing solid polymer electrolytes by soy protein‐based dynamic network. *Adv. Sci.* **2022**, *9*, 2103623.

Just Accepted

[166] Adjuik, T. A.;Nokes, S. E.; Montross, M. D. Biodegradability of bio‐based and synthetic hydrogels as sustainable soil amendments: A review. *J. Appl. Polym. Sci.* **2023**, *140*, e53655.
[167] Wang, H.;Zhou, A.;Hu, Z.;Hu, X.;Zhang, F.;Song, Z.;Huang, Y.;Cui, Y.;Cui, Y.; Li, L. Toward simultaneous dense zinc deposition and broken side‐reaction loops in the Zn//V2O5 system. *Angew. Chem.* **2024**, *136*, e202318928.
[168] Zhang, H.;Gan, X.;Gao, Y.;Wu, H.;Song, Z.; Zhou, J. Carboxylic acid‐functionalized cellulose hydrogel electrolyte for dual‐interface stabilization in aqueous zinc‐organic batteries. *Adv. Mater.* **2025**, *37*, 2411997.
[169] Chen, M.;Chen, J.;Zhou, W.;Han, X.;Yao, Y.; Wong, C. P. Realizing an all‐round hydrogel electrolyte toward environmentally adaptive dendrite‐free aqueous Zn–MnO2 batteries. *Adv. Mater.* **2021**, *33*, 2007559.
[170] Park, M.;Chung, K.;Kim, S.; Lim, J. Y. Label-free surface-enhanced Raman spectroscopy sensing with 3D-Printed Ag-coated Au nanorod microneedles: A Langmuir–Blodgett strategy for on-site pH monitoring. *Biosens. Bioelectron.* **2025**, 117848.
[171] Li, R.;Zhang, L.;Wang, X.;Wu, F.;Li, L.; Chen, R. A stretchable and self-healing polymer-in-salt all-solid electrolyte for wearable zinc-ion batteries. *Nano Res.* **2025**, *18*, 94907536.
[172] Li, H.;Han, C.;Huang, Y.;Huang, Y.;Zhu, M.;Pei, Z.;Xue, Q.;Wang, Z.;Liu, Z.; Tang, Z. An extremely safe and wearable solid-state zinc ion battery based on a hierarchical structured polymer electrolyte. *Energy Environ. Sci.* **2018**, *11*, 941–951.
[173] Luo, P.;Chen, R.;Liu, Q.;Li, X.;Yu, H.;Zhao, Y.;Wang, J.;Zhang, Q.; Zhao, Y. Highly Flexible and Structurally Stable Oriented Conductive Framework for Deformation‐Tolerant Zn‐Ion Batteries. *Adv. Funct. Mater.* **2025**, *35*, 2506742.
[174] Cui, D.;Sun, Y.;Li, T.;Hu, Z.;Zhao, Y.;Wang, X.;Chen, S.;Toktarbay, Z.; Wei, H. Mechanically robust polyacrylamide/gelatin ionic hydrogels reinforced by sodium alginate for wearable device applications. *Adv. Compos. Hybrid Mater.* **2025**, *8*, 233.
[175] Shao, Y.;Zhao, J.;Hu, W.;Xia, Z.;Luo, J.;Zhou, Y.;Zhang, L.;Yang, X.;Ma, N.; Yang, D. Regulating interfacial ion migration via wool keratin mediated biogel electrolyte toward robust flexible Zn‐ion batteries. *Small* **2022**, *18*, 2107163.
[176] Huang, J.;Chi, X.;Yang, J.; Liu, Y. An ultrastable Na–Zn solid-state hybrid battery enabled by a robust dual-cross-linked polymer electrolyte. *ACS Appl. Mater. Interfaces* **2020**, *12*, 17583–17591.
[177] Mao, Y.;Ren, H.;Zhang, J.;Luo, T.;Liu, N.;Wang, B.;Le, S.; Zhang, N. Modifying hydrogel electrolyte to induce zinc deposition for dendrite-free zinc metal anode. *Electrochim. Acta* **2021**, *393*, 139094.
[178] Liu, Z.;Wang, D.;Tang, Z.;Liang, G.;Yang, Q.;Li, H.;Ma, L.;Mo, F.; Zhi, C. A mechanically durable and device-level tough Zn-MnO2 battery with high flexibility. *Energy Storage Mater.* **2019**, *23*, 636–645.
[179] Li, Y.;Yang, Y.;Liu, X.;Yang, Y.;Wu, Y.;Han, L.; Han, Q. Flexible self-powered integrated sensing system based on a rechargeable zinc-ion battery by using a multifunctional polyacrylamide/carboxymethyl chitosan/LiCl ionic hydrogel. *Colloids Surf. A: Physicochem. Eng. Asp.* **2022**, *648*, 129254.
[180] Zhou, J.;Li, Y.;Xie, L.;Xu, R.;Zhang, R.;Gao, M.;Tian, W.;Li, D.;Qiao, L.; Wang, T. Humidity-sensitive, shape-controllable, and transient zinc-ion batteries based on plasticizing gelatin-silk protein electrolytes. *Mater. Today Energy* **2021**, *21*, 100712.

Just Accepted

[181] Wang, B.;Li, J.;Hou, C.;Zhang, Q.;Li, Y.; Wang, H. Stable hydrogel electrolytes for flexible and submarine-use Zn-ion batteries. *ACS Appl. Mater. Interfaces* **2020**, *12*, 46005–46014.
[182] Dong, H.;Li, J.;Zhao, S.;Jiao, Y.;Chen, J.;Tan, Y.;Brett, D. J.;He, G.; Parkin, I. P. Investigation of a biomass hydrogel electrolyte naturally stabilizing cathodes for zinc-ion batteries. *ACS Appl. Mater. Interfaces* **2020**, *13*, 745–754.
[183] Liu, Y.;Gao, A.;Hao, J.;Li, X.;Ling, J.;Yi, F.;Li, Q.; Shu, D. Soaking-free and self-healing hydrogel for wearable zinc-ion batteries. *Chem. Eng. J.* **2023**, *452*, 139605.
[184] Liu, C.;Xu, W.;Mei, C.;Li, M.;Chen, W.;Hong, S.;Kim, W. Y.;Lee, S. y.; Wu, Q. A chemically self‐charging flexible solid‐state zinc‐ion battery based on VO2 cathode and polyacrylamide–chitin nanofiber hydrogel electrolyte. *Adv. Energy Mater.* **2021**, *11*, 2003902.
[185] Qin, J.;Zhang, J.;Zhang, Z.;Tian, J.;Yuan, D.; Pan, J. H. Cu-doped δ-MnO_2 nanosheet assemblies with Pluronic F127 interface engineering for high-performance aqueous Zn-ion batteries. *J. Energy Storage* **2026**, *174*, 123053.
[186] Zhang, B.;Cai, X.;Li, J.;Zhang, H.;Li, D.;Ge, H.;Liang, S.;Lu, B.;Zhao, J.; Zhou, J. Biocompatible and stable quasi-solid-state zinc-ion batteries for real-time responsive wireless wearable electronics. *Energy Environ. Sci.* **2024**, *17*, 3878–3887.
[187] Yang, X.;Zhang, Z.;Wu, M.;Guo, Z. P.; Zheng, Z. J. Reshaping zinc plating/stripping behavior by interfacial water bonding for high‐utilization‐rate zinc batteries. *Adv. Mater.* **2023**, *35*, 2303550.
[188] Wang, Y.;Mo, L. e.;Zhang, X.;Ren, Y.;Wei, T.;He, Y.;Huang, Y.;Zhang, H.;Tan, P.; Li, Z. Regulating water activity for all‐climate aqueous zinc‐ion batteries. *Adv. Energy Mater.* **2024**, *14*, 2402041.
[189] Huang, L.;Cheng, H.;Huang, Z.;Xiong, Y.;Cai, X.;Wang, Y.-X.;Gao, Y.;Ge, J.;Zhang, J.; Ma, S. Enabling high-performance Zn–I 2 batteries with a solvation-regulating, ion-selective, and flexible sulfonic acid-water reducer gel electrolyte. *Nano Res.* **2026**, *19*, 94908379.

Just Accepted